Russian Chemical Reviews **72** (5) 375 – 391 (2003) © 2003 Russian Academy of Sciences and Turpion Ltd

DOI 10.1070/RC2003v072n05ABEH000795

Nanochemistry: a direct route to high technologies of the new century

A L Buchachenko

Contents

I.	Nanochemistry: a science about the 'nanoworld'	375
II.	Nanoclusters	377
III.	Nanotubes	379
IV.	Nanowires	384
V.	Nanomechanics	386
VI.	Technologies for handling nanoobjects	388

Abstract. This review deals with problems involved in creating and handling nanoparticles, as well as the integration of nanoparticles into various systems and the operation of such systems. The review analyses the chemical, electrical and magnetic properties of the three main elements of nanotechnologies, *viz*., clusters, nanotubes and nanowires. The bibliography includes 77 references.

I. Nanochemistry: a science about the 'nanoworld'

Chemistry celebrated the end of the 20th century with a remarkable result of strategic importance: it has approached the threshold of being able to detect a single molecule and identify its physical and chemical behaviour. As a result, a new field of chemistry has appeared, *viz* ., the chemistry of single molecules. A molecule acquires identity and becomes a 'person'.[1–3]

This new field defines precisely the upper boundary of yet another field of chemistry, called nanochemistry, which studies small ensembles of molecules (or atoms) comprising more than one species. However, there is no strict quantitative criterion for defining the lower boundary of this region; furthermore, setting any artificial limits (*e.g*., size in nanometres or number of molecules or atoms in hundreds or thousands) is harmful.

The world of nanochemistry is a vast world from individual molecules to continual systems that constitute a phase. Nanoparticles are characterised by intermolecular interactions that deprive molecules of their personality; the properties and behaviour of molecules in ensembles differ from those of single molecules (social communities of people and animals show some similar features).

The main and fundamental problem of nanochemistry around which all interests of researchers are concentrated is the problem of dimensional effects. The intriguing questions are: how the properties of single molecules evolve into the properties of a phase when molecules are united; how bridges between the world of single molecules and the macroscopic world of substance are built; how the hierarchy of quantity is converted into the hierarchy of properties. Dimensional effects are so diverse and unexpected that there is no general solution to the problem. The methods of quantum chemistry and molecular dynamics succeed in answering specific questions only. They can explain almost everything but cannot provide reliable predictions. However, science only then becomes real science when it can foresee. In this sense, nanochemistry altogether is still ahead of us; nanoparticles will long remain our 'employers'.

The lower boundary of nanochemistry (with the adjoining colloid chemistry and chemistry of highly dispersed systems) is rather vague and is determined by common sense, which appeals to two important considerations: first, the relationship between the concepts 'nanoparticle' and 'nanoreactor' (*vide infra*); second, the extent to which nanoparticles lose their individual properties when materials or colloid systems are formed from them, *i.e*., how much they lose their identity as 'chemical persons'.[4]

1. The structural-chemical contours of nanochemistry

The simplest nanoreactors in which reagents are arranged spatially are van der Waals molecules, *i.e*., weakly bound complexes of atoms, radicals, ions and molecules; the partners in such complexes are held by intermolecular non-valence interactions. The van der Waals molecules have been observed in supersonic molecular beams and studied by laser and microwave spectroscopy and by mass spectrometry. Very many molecules of this kind are known: He_2, $(H_2)_2$, $C_6H_6 \cdot CH_4$, $C_2H_4 \cdot Ar$, $HCl \cdot Xe$, $Ar \cdot I_2$, CaMg, $(C_2H_2)_2$, $He \cdot NH_3$, *etc*. Various physical parameters have been determined for the majority of these molecules: symmetry and geometry (bond angles and lengths), dipole moments, rotation and oscillation frequencies, lifetimes and dissociation energies, magnetic susceptibilities and ionisation potentials, quadrupole and coupling constants and many others.

But why are van der Waals molecules so interesting to physicists and chemists and what are they good for? First, they are a reliable source of atom – atom potentials; it is due to them that interatomic potentials have acquired spectroscopic precision and are now widely used as the key parameters in calculations of chemical and molecular dynamics of liquids, glasses and macromolecules; they are used in calculations of intermolecular energy transfer and energy relaxation. Atomic potentials are responsible for the molecular organisation of crystals and macromolecules, polymorphism of crystals, self-organisation of molecular ensembles, self-replication of biomolecules, *etc*.

Second, van der Waals molecules are responsible for the macroscopic properties of gases (*PVT* diagrams, viscosity, second virial coefficient, *etc*.); they induce condensation, crystallisation

A L Buchachenko N N Semenov Institute of Chemical Physics, Russian Academy of Sciences, ul. Kosygina 4, 119991 Moscow, Russian Federation. Fax: (7-095) 938 24 84. Tel. (7-095) 939 71 28

Received 11 November 2002
Uspekhi Khimii **7** (5) 419 – 437 (2003); translated by S S Veselyi

and other phase transitions; they also define the critical points of substances and the density fluctuations and correlation radii in these points.

Do the van der Waals molecules play any role in chemical reactions? At first glance, the answer should be 'no', since the bond energy between the partners in these molecules is low, *viz*., about kT or sometimes even lower. However, a partner in such a molecule may act as a 'rider', *i.e*., as a third body that acts as a drain for the excess of energy evolved in the reaction, and eliminate reaction prohibition as regards the orbital symmetry or angular momentum. Here is a good example:

$$Cl_2 + Br_2 \longrightarrow 2\,ClBr.$$

The cross-section of this reaction is negligibly small due to an orbital symmetry forbiddenness. However, the same reaction between $(Cl_2)_2$ (a van der Waals molecule) and Br_2 occurs in almost each collision, since orbital symmetry forbiddenness is eliminated by the third particle.

It is known that the angular distribution of products in reacting molecular beams suggests unambiguously that many reactions (even $H + D_2 \rightarrow HD + D$) are preceded by the formation of short-lived complexes between the reagents, *i.e*., the van der Waals molecules, which can often be observed spectroscopically.

The interest in complexes between metal atoms and small molecules (H_2, CO, CH_4, C_2H_4, N_2, *etc*.) is increasing continuously; many complexes of this kind have already been studied to date: $Al\cdot N_2$, $Ca^+\cdot\ N_2$, $Hg\cdot N_2$, $Cr^+\cdot N_2$, *etc*. Pair non-valence interactions of atoms and molecules are at the upper boundary of nanochemistry.

In addition to the van der Waals molecules, there is an enormous number of other nano- and microreactors of diverse nature, scale and molecular ordering: complexes; crystal solvates; nanohydrates (*e.g*., that of methane); clathrate compounds (*e.g*., with cyclodextrins, semispherands and calixarenes as 'hosts' which interact with guest molecules); macromolecules (helices or rigid rods); cavities in zeolites and porous materials. Many characteristics are different in microreactors: molecular dynamics of reagents, mechanisms and rates of chemical transformations, pK values of acids and bases, local charges and their distribution, potentials and electron affinity, conformations and reactivity; new 'forced' reactions appear, and many other anomalies are found.

The area of nanochemistry which aims at the creation of closed or semiclosed nano- and microreactors is being developed rapidly. Methods to obtain polymers in which 75% of the volume is occupied with monodisperse empty spheres have been developed; the volumes of these spheres can be varied from 10 to 10^3 nm. Molecular 'vases' have been created, *i.e*., calixarenes which can reversibly 'captivate' guest molecules and release them (depending on the solvent, solution pH and calixarene structure);[5] molecular traps have been synthesised, *i.e*., carseplexes that can trap molecules like certain predacious insect-catching flowers. Unlike endofullerenes, they can release their molecular 'preys' after a change in the solvent, pH, *etc*. All these structures belong to the class of molecular containers or self-folding cavitands which can trap predefined molecules and release them as the conditions are changed.

'Empty' tubular silicon fibres, *viz*., unidimensional nanoreactors, have been created. They are obtained by deposition of tetramethyl orthosilicate dissolved in supercritical CO_2 onto carbon fibres. Carbon is removed by thermal treatment in O_2 or by plasma etching to give nanotubular silicon fibres ready for various uses, *e.g*., as nanoreactors or nanocontainers. The diameter of such fibres is determined by the diameter of the carbon fibre and is an order of magnitude larger than that of carbon nanotubes.

The interest in such well-known nanoreactors as micelles has not slackened, either. Dendrimeric megamolecules are also widely used as nanoreactors and nanocontainers.

Novel unusual quasi-bidimensional nanoreactors have recently been synthesised, *viz*., rigid graphite-like planes connected by flexible-chain bridges ('columns') consisting of carbon (polymethylene) chains. The distances between the graphite-like planes in such reactors can be varied by changing the number of atoms in a 'column' (*e.g*., C_{10}, C_{16}, *etc*.); the lateral distances between the columns can be changed by varying the number of columns (the thickness of the column 'forest'). The reversible and continuous contraction – expansion of the interplanar distance is achieved by the stimulation of conformation transitions in polymethylene chains, *viz*., from a coil conformation (the planes are spaced most closely) to a stretched chain (the most widely spaced planes).[6] These transitions can be smoothly controlled by adjusting the nanoreactor to a given volume by filling it with solvents. Such a system is similar to a 'bellows' system; its reversible contraction – expansion mimics muscular contraction. It may be considered as an ideal reversible mechanochemical molecular machine. It can be used as a nanoreactor by loading with catalysts and carrying out catalytic reactions; it can also serve as a versatile and reversible molecular container, *etc*. The first system of this kind was based on a decane-1,10-diphosphonate derivative of γ-zirconium phosphate.

A 'contour' analysis of nanochemistry reveals two facets: on the one hand, nanochemistry produces its own objects, *viz*., nanoparticles, nanoreactors, nanocontainers; on the other hand, it employs the numerous advantages of nanoparticles and their unusual and flexibly adjustable properties for its own needs, such as the development of new materials, reagents and elements for use in nanotechnologies.

2. A nanoparticle and a nanoreactor

Every year, nanochemistry becomes an increasingly structured science with strictly defined concepts and formulated terminology, the language as 'the dress of thought'. In view of this, it is necessary to define two key concepts, *viz*., the nanoparticle and the nanoreactor. The former concept characterises the dimensional parameters, while the latter defines the nanoparticle function. For example, an iron cluster loses its specific functional properties (ionisation potential, magnetism) almost completely and approaches the properties of metallic iron when the number of atoms in the cluster (n) equals 15. At $n > 15$, it remains a cluster in terms of dimension, but it loses the properties of a 'nanoreactor' in which the properties become a function of the size. In those clusters where an α-naphthol molecule is surrounded by n water molecules, a cluster behaves as a nanoreactor at $n \leqslant 20$; its properties depend on its size. At $n > 20$, this dependence disappears and the cluster behaves as a macroscopic aqueous 'reactor' in which the reagent is localised; however, it does not display any chemical anomalies. For example, at $n > 20$, acid dissociation of α-naphthol and proton transfer to water molecules occur.

In clusters of monovalent magnesium (and calcium) with $(H_2O)_n$ and $(CH_3OH)_n$, the electron transfer and hydrogen reduction occur according to the reactions

$$Mg^+(CH_3OH)_n \longrightarrow (MgOCH_3)^+(CH_3OH)_{n-1} + H,$$

$$Mg^+(H_2O)_n \longrightarrow (MgOH)^+(H_2O)_{n-1} + H$$

only in the range $6 \leqslant n \leqslant 15$; no hydrogen evolution occurs for any other n values.[7]

Hence, the cluster demonstrates its dimensional effects and 'works' as a nanoreactor only at $n \leqslant 15$; at $n > 15$, the cluster behaves as a small reaction vessel without dimension-related anomalies in its reactivity.

Nanocavities in various porous materials may be considered as nanoreactors as long as the properties of the reagents which they incorporate (pK, ionisation potential), their structures (conformations) and properties of the reacting systems (rate constant, 'forced' reactions, molecular dynamics, *etc*.) depend on the cavity size. When these dependences do not exist any more, nanocavities

become just nanosized containers in which the trapped particles behave as if they were located in an infinite volume.

Of course, the nonequivalence of the concepts 'nanoparticle' and 'nanoreactor' is not always obvious; in many cases, it is impossible to distinguish them. However, it is important to perceive clearly the two aspects of the dimensional effect, both as a purely scale- and space-related effect and as a physicochemical phenomenon where the size affects the properties of trapped atoms and molecules. It is this second aspect that is the most attractive feature of nanochemistry.

3. Nanoclusters, nanowire and nanotubes: three key objects of nanotechnologies

The diversity of nanoobjects studied by nanochemistry is enormous (see the section about the contours of nanochemistry); the chemistry of these nanoobjects is equally diverse. However, we will consider only those nanoobjects which either already show real promise for the high technologies of the new century or which may ensure serious breakthroughs in the future, *viz*., in the creation of nanolasers, nanocables, optical nanoconverters and nanosources, nanoelements of integrated circuits, nanocatalysts, nanomechanical devices, nanoresonators, nanowave guides, nanodiodes, *etc*. These objects include three-dimensional clusters, quasi-unidimensional clusters (nanowires) and nanopipes. It is these objects that may ensure extreme, almost on the molecular scale, miniaturisation of diodes, transistors and other elements of nanoelectronics, nanomechanics, nanophysics, nanoinformatics (nanocomputers, nanosensors), *etc*.

II. Nanoclusters

1. A cluster as a nanoreactor

The diversity of nanoclusters is infinite, and therefore they are inexhaustible. They can be neutral (atomic and molecular) or charged (ionic and molecular ionic). They are obtained and studied in gases (*e.g*., in expanding supersonic molecular atomic beams), in zeolite channels (*e.g*., the In_8 cluster), in liquids (including liquid helium), on solid surfaces, in solid matrices, *etc*. Clusters are extremely important in chemical materials science (cluster materials with unusual physics and mechanics), in chemical analysis and in diagnostics (detectors and sensors).

Clusters are relatively new objects in chemistry; they are studied by organoelement and organometallic chemistry and by chemical physics (atomic and molecular clusters). Many studies have dealt with the methods of their synthesis, their structures and properties. Their role in condensation, evaporation and crystallisation processes is also critical; they serve as precursors of new phases ('protophases'). However, it is the chemistry of these species, their reactivities, catalytic 'potential' and direct use in materials science that attracts the greatest interest. Cluster chemistry belongs to the future.

The rate of photoinduced isomerisation of a *trans*-stilbene molecule in a $(hexane)_n$ cluster was measured by picosecond spectroscopy in molecular beams.[8] The isomerisation rate constant decreases with an increase in n in the order: 9.7×10^9 ($n = 0$, free molecule); 3×10^9 ($n = 1$); 1×10^9 ($n = 2$); 0.8×10^9 ($n = 3$); 0.5×10^9 s^{-1} ($n = 4$) to reach a limit at $n \geqslant 5$. Unexpectedly, all of these constants turned out to be smaller than the observed isomerisation constant of *trans*-stilbene in pure liquid hexane at the same temperatures and energies (11.5×10^9 s^{-1}). Thus, incorporation of a *trans*-stilbene molecule in a cluster decreases its reactivity. The cluster shell traps the molecule more strongly than the 'liquid-phase' shell: the former anomalously increases the kinetic (Kramers') friction, *i.e*., the movement of a reacting molecule on the potential surface along the reaction coordinate.

The abundance and hence importance of clusters may turn out to be even greater than it seems now. It has recently been discovered experimentally (by cold neutron scattering and XRD) that liquid ammonia consists of $(NH_3)_7$ clusters where one molecule is located in the centre while the remaining molecules are located at the periphery. The cluster structure of water is well known: water molecules are combined into hexa-, penta- and tetramers to give structures with similar energies resembling a prism, a cage, an 'open book', adamantane, as well as dodecahedra and other large clusters. Even liquid solutions of ethanol in water are inhomogeneous: they consist of coexisting water and alcohol clusters;[9] the fractions of these clusters become equal when the alcohol content in water is about 40%. It is possible that the particular qualities of this water–alcohol solution originate from this fact. Liquid benzene was also found to have a cluster structure. It looks like this is a general phenomenon; in such cases, all liquid-phase reactions should be interpreted as reactions in nanoreactors.

What is more, a chemical reaction itself may favour the organisation of molecules into nanoreactors. For example, a colourless spiropyran with a long hydrocarbon 'tail' is converted photochemically into a coloured bipolar compound with separated charges; it is the molecules of this compound that are combined into micelles. Here, the photochemical reaction works as a trigger that switches micelling on.

A new trend in cluster chemistry is the study of the reactions of clusters with solids as a function of cluster energy. The elasticity of a cluster upon collision with a surface turns out to be very high. As is exemplified with $H^+(H_2O)_n$, $H^+(CH_3OH)_8$, $(C_6H_5CH_3)_5^+$ and $H^+(NH_3)_{10}$ ionic clusters and the diamond surface, clusters are reflected elastically from the surface and retain about 75% of their initial energy. The high elasticity of a cluster is explained by its high entropy (owing to the participation of different isomers in the molecular structure of the cluster).

However, when cluster ions acquire a high energy above a certain threshold, they disintegrate (mainly into monomeric fragments). In particular, $H^+(NH_3)_{10}$ disintegrates into NH_3 molecules faster than 80 ps. This suggests that fast energy redistribution occurs in such a 'superheated' cluster. Yet another remarkable phenomenon is the impact-induced chemical reactions in clusters [*e.g*., the formation of I_2^- from the cluster ions $(CH_3I)_n^-$ and F_2^- from $(CH_3F)_8^-$]. This new direction is called the femtosecond cluster mechanochemistry.[10]

2. Clusters in catalysis

The importance of cluster materials in catalysis was recognized long ago, and intense development in this field is continuing.[11] However, the technological capabilities of cluster catalysis are much greater than the achievements: this is an iceberg the major part of which has not yet been explored.

There are two main circumstances that are promising for the technological application of cluster catalysis: the high surface area of catalysts (which is related to productivity) and dimensional effects, which manifest themselves in the properties of clusters as nanoreactors (this is related to the selectivity and possibility of 'tuning' a cluster for a specific reaction). As indicated above, a general solution to the 'dimensional' problem is unknown; because of that, clusters continue to remain mysterious objects. Their route to catalysis starts from testing their reactivities in model experiments. In particular, any cluster of any size can be prepared in molecular beams, and reactions of these clusters with added molecules can then be studied by mass spectrometry.

It was shown using this method that the Re atom does not react with CH_4, whereas the Re_3 cluster is reactive. Linear three-atom Cu_3 and Ni_3 molecules do not react with H_2 and CH_4, whereas triangular molecules are highly reactive (the Ni_{13} cluster is also very reactive). The Co_n clusters react with H_2 in a dissociative way upon virtually each collision if $n = 3$, 4, 5 or 10–18, whereas clusters with $n = 6$–9 are completely inert.[12]

Figure 1 shows the dependence of rate constants on the cluster size n for the reactions $Nb_n + D_2$ and $Nd_n + N_2$. One can see a distinct stepwise dependence of reaction rates (dissociative adsorption of N_2 and D_2 molecules on an Nd_n cluster is the rate-determining step) on the size of the cluster; it is almost the same for both reactions and is insensitive to temperature. On the other

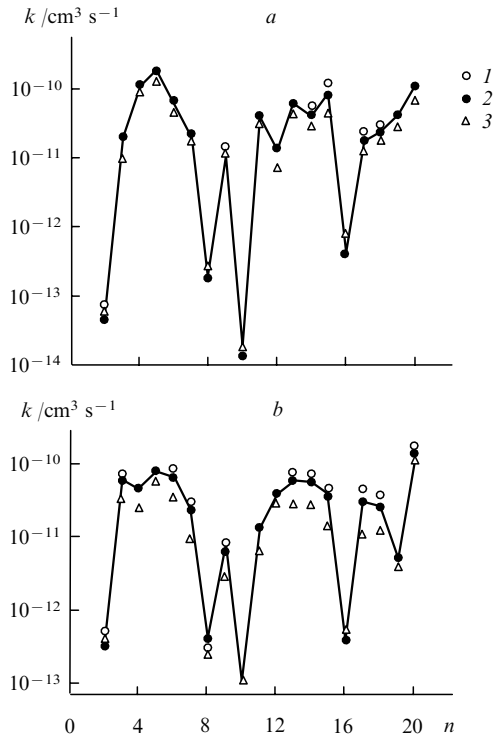


Figure 1. Dependence of the rate constants of dissociative adsorption of D_2 (*a*) and N_2 (*b*) on the size of a niobium cluster (*n* is the number of atoms in the cluster).
Temperature /K: (*1*) 280, (*2*) 300, (*3*) 370.

hand, the rate constant for the reaction of Nb_n with O_2 [$(3-7)\times10^{-10}$ cm^3 s^{-1}] is similar to the constant of bimolecular collisions and does not depend on *n* (the dimer Nb_2 is an exception).[13]

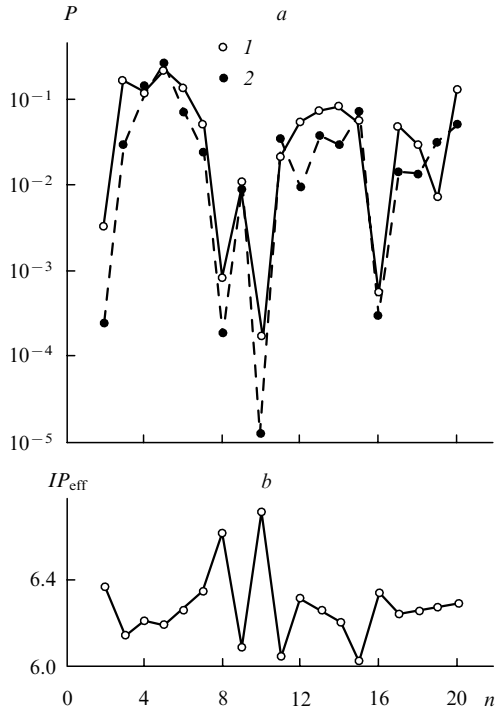


Figure 2. Dependence of the probability of the reactions $Nb_n + D_2$ (*1*) and $Nb_n + N_2$ (*2*) at 300 K (*a*) and of the ionisation potential of the Nb_n cluster (*b*) on the size of the cluster.

Figure 2 displays two relationships: the probability of the reactions $Nb_n + D_2$ and $Nb_n + N_2$ and the ionisation potential of the Nb_n cluster as functions of *n*. A pronounced and unambiguous 'antiphase' relationship between the reactivity of clusters and their ionisation potentials is observed: the lower the ionisation potential IP_{eff} of a cluster the higher its reactivity. It was concluded on this basis that charge transfer between a cluster and an adsorbed molecule is the main factor that governs the cluster reactivity; it is this factor that is responsible for the dimensional effects in Nb_n clusters.[13] It is noteworthy that only the clusters with $n = 5$, 6 and 11 are reactive in the dehydrogenation of benzene.

The Mo_n clusters are highly reactive in the reaction with N_2 (dissociative adsorption). At $n = 16$ and 23, the reaction constant is close to the gas-kinetic threshold; at any other *n* values, the rate constants are two orders of magnitude lower.[14] The W_n clusters react similarly: the maximum reactivity is observed for clusters with $n = 16$ and 23.[15]

Even gold loses its chemical 'nobleness' in clusters. Figure 3 demonstrates the catalytic activity of Au_n clusters in the reaction

$$CO + O_2 \longrightarrow CO_2.$$

One can see that clusters with $n = 8$, 11, 15 and 18 are the most active.[16]

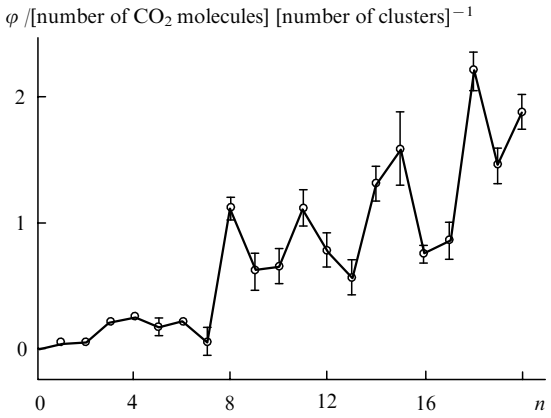


Figure 3. Yield of CO_2 molecules per cluster in the catalytic reaction $CO + O_2 \rightarrow CO_2$ as a function of the size of the Au_n cluster.

The MoO^+ ion does not react with NH_3; however, the ionic clusters $Mo_3O_8^+$ and $Mo_3O_9^+$ vigorously dehydrogenate ammonia to give a complex with the dehydrogenation product, *viz*., nitrogen; they also oxidise CO into CO_2.[17] The $V_3O_7^+$ cluster is very efficient in the dehydrogenation and cracking of butane, butene and butadiene; the $V_3O_{12}^+$ cluster has low activity, whereas $V_3O_{17}^+$ is totally inert. The $V_3O_6^+$ and $V_3O_{11}^+$ clusters are inefficient in these reactions but are actively involved in oxidative condensation and cyclisation, *i.e*., removal of only one oxygen atom from the cluster completely changes the type of the reaction involving the cluster.[18]

Studies on the use of titanium dioxide (TiO_2) as a photocatalyst for water and air purification from organic pollutants are under way. The drawback of TiO_2 is that its optical absorption band lies in the UV region (shorter than 390 nm), which decreases considerably its potential as a photocatalyst. Doping of TiO_2 with nitrogen (both in films and in clusters) shifts the $TiO_{2-x}N_x$ absorption band to the region of 520 nm, thus increasing considerably the efficiency of photocatalysis.

The dependence of the catalytic activity and reactivity of clusters on the dimensional effect follows, first, from the energetic parameters (the role of the ionisation potential in the reactivity of Nb_n clusters has already been noted above) and, second, from the structural changes in the atomic surfaces of clusters (exit of elements of different faces, edges and terraces on the surface). It

is the second reason that determines the difference in the reactivity of different faces of a single crystal in heterogeneous catalytic processes.

It has become clear now that the dimensional effects in catalysis are second in importance (the chemical nature of the catalyst is the most important). They can control both the rate (which can be changed by a few orders of magnitude) and the direction of a reaction.[19]

It should however be admitted that clusters as such are not catalysts yet. The use of high technologies in catalysis implies that clusters are tested for reactivity in specific reactions chosen with respect to reactivity and selectivity and finally combined in a macroscopic catalytic ensemble without losing the individuality of the clusters. The latter problem is not easy; many research groups are working towards its solution. Although it is unlikely that a general solution to this problem can be found, it can, in principle, be solved in each particular case.

A new strategy in heterogeneous catalysis involves a combination of catalysis with tunnelling scanning microscopy. The tip of a tunnelling microscope can deposit any number of atoms (including single atoms) onto any topological element of a surface (face, edge, terrace), thus creating catalytic nanoreactors and making it possible to test any reactions on them. The creation of an 'atomic pump', *i.e.*, prototype of a machine that deposits single atoms which drift through a nanotube, is a brilliant breakthrough that may occur in this nanotechnology. The drift of atoms is controlled by a laser (see Section IV.3). This is a new direction in the fundamental science of catalysis and a direct route to the use of high technologies in catalysis.

3. Optical converters

Particularly impressive are dimensional effects in semiconducting nanocrystals with sizes smaller than the Bohr exciton radius. In such nanoclusters (called quantum points), the quantum trapping of an electron-hole pair (photochemically or radiation-induced) in a restricted volume results in the expansion of the forbidden band as the cluster size decreases. This means that recombination luminescence shifts to the blue region (high energies) with a decrease in the cluster size. The CdSe nanocrystals 'dressed' in one or two ZnS monolayers represent a good example. If the diameter of the internal CdSe nucleus is changed stepwise from 23 to 55 Å, the bright blue luminescence changes to green, yellow, orange and finally bright red.[20] Upon coherent excitation of the electronic gas, gold clusters (nanorods) fluoresce with a quantum yield 10^6 times higher than metallic gold; furthermore, the quantum yield is proportional to l^2 (where l is the nanorod length), while the maximum of the luminescence band is proportional to l. It has been shown recently that a carbon nanotube is also a quantum point.[21]

Quantum points are mainly studied by physicists. The creation of quantum points doped by admixture ions is a subject of nanochemistry. In doped quantum points, the excitation energy 'mounts' the admixture site and is emitted by it. For instance, high-quality nanocrystals of ZnSe doped with Mn^{2+} ions were obtained by a reaction of a solution of selenium in trioctylphosphine with diethylzinc and dimethylmanganese.[22] In this case, each nanocrystal contained one Mn^{2+} ion. Using the magnetic circular dichroism and electron spin resonance, it was proved that the Mn^{2+} ion is located inside the nanocrystal, replacing the Zn^{2+} ion in the cubic lattice of ZnSe. It should be noted that such perfect doped nanocrystals could not be obtained when diethylmagnesium was used instead of diethylmanganese; the Mg^{2+} ions were partially located on the surface and distorted the optical conversion.

The blue fluorescence characteristic of undoped crystals is suppressed almost totally in manganese-doped ZnSe nanocrystals and is changed for red fluorescence (2.12 eV, 585 nm); the quantum yield of luminescence at 293 K is 22% and reaches 75% below 50 K. Thus, the admixture Mn^{2+} ion in semiconductor crystals is a collector of the electron–hole recombination energy and its efficient monochromatic emitter.

Of light-converting organic nanoclusters, J-aggregates are very popular, *i.e.*, ensembles of molecules of organic dyes which efficiently collect the electron excitation energy (directly or through electron–hole recombination) and emit it with a high quantum yield (as a rule, in a narrow spectral region). In fact, they act like molecular antennae in photosynthetic centres.

4. Magnetism and spintronics

Because the ratio of the surface and bulk atoms in ferromagnetic metal clusters is finitesimal, the mutual compensation of the atomic magnetic moments of clusters is incomplete. Furthermore, the crystal lattice of the cluster can differ from that of the metal. For this reason, the magnetization and magnetic atomic moment in clusters depend on the cluster size and differ from the macroscopic characteristics of the metal. Based on this, new nanocluster magnetic materials with new attractive properties are created. This field of research has been successfully developed for a long time; good books and reviews on the topic are available (see, *e.g.*, Refs 23 and 24), which allows us to refrain from discussing it here.

Over the past three years, a new field of electronics, *viz.*, spintronics (spin electronics), has developed rapidly. Spintronics opens up new horizons for developers of new-generation electronic devices and instruments using high technology.[25] Unlike classical electronics, which controls the movement of electrons and holes (negative and positive charges) by means of potentials (both biasing and stopping potentials), spin electronics controls both charges and spins (magnetic moments) of current carriers. Two controlling factors work in spintronics, *viz.*, electric potentials and magnetic fields.

The main material of spintronics is represented by either a film of a conducting metal (copper, ruthenium) enclosed between layers of ferromagnetic metals or a semiconductor nanometre-thick film separating ferromagnetic layers. Owing to the magnetic resistance effect, the electric current in a film of a non-magnetic metal or the tunneling current in a semiconductor film (tunnel barrier) depends not only on the controlling electric potentials but also on the magnetic field created by the ferromagnetic layers and the external field. Clearly, this circumstance increases considerably the number of methods to monitor and control electric currents by both selecting ferromagnetic films (with different hysteresis loops and different magnetisations) and by applying an external magnetic field. In combination with controlling potentials, this creates a flexible and multiparameter system for the control of electric currents.

Currently, there is a race to create new technologies and devices using spintronics; the tension of this race is only comparable to that of the 'cold cheminuclear synthesis' race at the end of the 1980s. However, unlike cold cheminuclear synthesis, spintronics is realistic. The development of many devices is underway, including spin-dependent field transistors, spin-dependent light-emitting diodes, spin tunnel diodes and optical switches in the terahertz frequency range, spin modulators, coders and decoders, spin-dependent sensors and elements of computer and communication memory, *etc*. Practical Americans estimate the new technology market to be worth multi-trillion dollars;[25] certainly, nanochemistry is the main paradigm of these new developments.

III. Nanotubes

The chemistry and physics of nanotubes are under rapid development. Many methods and technologies for the synthesis of these species have been developed, *viz.*, electric-arc discharge, laser-thermal ablation, flame synthesis and pyrolysis of hydrocarbons.[26] As of today, the best one is the pyrolytic method for the synthesis of nanotubes from CO, CH_4, C_2H_4 or C_2H_2 on a surface with a deposited catalyst or with a volatile catalyst precursor [like $Fe(CO)_5$]; in the latter case, the synthesis of the catalyst (*e.g.*, Fe

atoms and clusters) and the synthesis of the nanotubes are coupled. The combination of these diverse methods is the essence of the technology of chemical deposition from a gas (or vapour) phase on a solid surface (support), the technology which is considered the most efficient today. Methods for the continuous and large-scale production of nanotubes with controlled growth rate and adjustable diameters and lengths have already been developed.[26]

1. Architecture of nanotubes

For nanotubes as technological objects, the architecture of their ensembles and the possibility of controlling it, adjusting it and combining objects into integrated circuits are important factors; the latter factor makes the problem of nanocontacts particularly important.

Considerable success has been achieved in the creation of controlled architecture. Multilayered tubes with preset architecture were obtained using a porous silicon support with submicron pores electrochemically pretreated (electrocutting) in an HF – MeOH solution. This treatment has made it possible to create a thin nanosized layer with nanopores (diameter about 3 nm) on silicon. Atop this nanolayer, a catalyst (iron film 5 nm thick) was sputtered through a shading mask. Subsequently, nanotubes were synthesised from ethylene at 700 °C by chemical deposition onto catalytic islands. The multilayered nanotubes formed on these islands looked like a thick forest of perfect 'towers' oriented strictly vertically. The length of the nanotubes (height of the 'towers') was controlled in the range 10 – 240 nm; the square of a 'tower' depended on the mask selected.[27]

The reason for the architectural perfectness of the 'nanopipe' ensemble (and the advantage of the technology) is that the catalyst is strongly retained in the nanopores of the support, while the strong van der Waals interaction of the outer spheres of the growing nanotubes precludes their distortion and ensures the rigid fixation of the entire bunch of nanotubes growing on a single catalytic island. It was found that the growth of nanotubes on nanoporous silicon occurs much faster than on 'non-cut' planar silicon. The reason for the fast growth of nanotubes is that ethylene arrives at the catalytic islands not only from the gas phase but also through the nanopores of the support, 'feeding' the growing nanotubes with carbon from the inside. Finally, yet another remarkable result of this technology is the synthesis of nanotubes with monodisperse diameters.[28]

Monolayer nanotubes are usually grown by arc discharge or laser ablation. In these cases, the evaporation of carbon atoms occurs at 3000 °C or higher, which restricts the growth of nanotubes; they bend and get entangled, and it is difficult to purify them and build ensembles from them. High-quality monolayer nanotubes are obtained by chemical deposition of carbon from methane. The advantage of methane is that its stability precludes the formation of amorphous carbon that contaminates the catalyst on which nanotubes grow.

A bimetallic Fe/Mo catalyst deposited on an aluminium – silicon material prepared by sol – gel technology was found to be the best catalyst for the synthesis of monolayer nanotubes. The diameters of the nanotubes grown on this catalyst range from 0.7 to 1.5 nm (this is their disadvantage); the tubes with a diameter of 1.4 nm are obtained in a maximum yield. Again, the main condition required to obtain high-quality nanotubes is a strong bond between the metal and the support. The high porosity of the support ensures a high density of catalytic sites on the surface and the easy access of methane to these sites. The latter circumstance is particularly important, since the growth rate of nanotubes is limited by gas diffusion.

It is important for nanotechnology that oriented nanotubes can be grown. The first steps in this direction have already been made. Lithographic methods are used to create islands (elevations with deposited catalyst 'chips') on supports. Nanotubes grow on such chips; many of them start from one chip and reach another one thus creating a network of suspended 'bridges' between the islands. The architecture and density of the network is set by the initial architecture of the deposited chips. This may already be regarded as a prototype for integrated circuits.[28]

The diameters of nanotubes obtained by chemical deposition are determined by the size of the catalytic cluster or the nanopore in which the catalyst is 'sitting', whereas those of the nanotubes obtained in an arc discharge are determined by the pressure of the inert gas (helium). It has recently been shown[29] that the mean diameter of nanotubes formed in an arc discharge increases proportionally to the logarithm of pressure. This result may prove to be useful.

2. Architecture of nanocontacts

Nanocontacts are the trouble spot of nanotechnologies. Based on current experience, two approaches to the formation of nanocontact architecture seem possible: by different growth mechanisms of nanotubes and by handling nanotubes (this will be explained below).

The growth mechanism may be judged from the state of the nanotube ends (they are usually visible under an electron microscope). When catalyst species are strongly fixed on a support, the ends of the growing nanotubes are free of catalyst species, hollow and covered with hemispheres (fullerene caps). In such cases, tubes grow from their bases: through adsorption and decomposition of methane (or some other carbon source) on the surface of the metal catalyst, dissolution of carbon and diffusion of carbon atoms to the metal surface layer, oversaturation of the solution with carbon and deposition of carbon on the lower part of a tube. A tube grows from its bottom (base); carbon arriving from the catalyst builds the ground floor of the tube and 'pushes' it upwards. In this case, a strong nanocontact of the tube with the prepared support, where the required architecture of nanotube chips has been preset, is formed at once.

It is possible to update this technology by feeding the catalyst from the gas phase; in such a case, catalyst nanoclusters 'mount' the top of the tube and growth continues on them.

A brilliant version of this technology has been implemented recently.[30] Nanotubes were grown on a quartz surface at 800 °C in a stream of an Ar/H_2 mixture to which drops of a solution of ferrocene in xylene were injected at regular intervals. Pyrolysis of ferrocene was accompanied by the formation of iron clusters which were deposited on quartz at the very beginning of the process. Xylene decomposed on these nanocontacts and carbon tubes started to grow there. New clusters formed on the tops of the nanotubes from subsequent portions of ferrocene and xylene, and the tubes continued to grow on these clusters. This process gives rise to a colony of nanotubes. It resembles a multistorey building: there are catalyst clusters in the base and between the storeys, whereas the distance between the storeys determined by the intervals between the injection of ferrocene + xylene portions is occupied by nanotubes.

Figure 4 demonstrates the architecture of the resulting nanotubes. The image on the left, obtained using a scanning electron

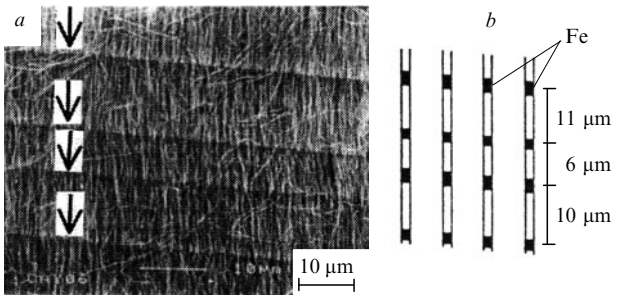


Figure 4. An electron-microscopic image of colonies of nanotubes grown on iron clusters (*a*) and a schematic drawing of tubes with incorporated iron clusters (*b*).

microscope, shows a colony of vertical nanotubes. The horizontal parallel lines (bridges between the storeys) correspond to the iron clusters which are formed at the moments when the solution of ferrocene in xylene is injected. If the intervals between the injections are constant, the 'storeys' grow strictly uniformly and have equal heights. Furthermore, the height of a storey depends on the ferrocene : xylene ratio in the solution which feeds the growth of the nanotubes. This ratio also affects the tube growth rate, because in fact it is the catalyst : carbon ratio.

This technology is remarkable because in this case iron clusters are included in the growing tube so that the catalyst is captured inside the tube and is in a strong contact with the tube wall from the inside (this is sketched in Fig. 4 *b*). The growing tube shapes the cluster in such a way that it becomes oblong; the cross-section of the cluster exactly matches the inner diameter of the tube (this has been proven by transmission electron microscopy [30]). What is more, the nanotube reliably protects the trapped iron clusters from oxidation. The nanotubes obtained by this method have ferromagnetic properties, which allows one to handle them using magnetic fields and magnetic manipulators. The architecture of such an ensemble of nanotubes resembles that of a macroscopic crystal in which the lattice points are occupied by iron clusters included in nanotubes with a preset space periodicity.

Clearly, this technology offers ways to create nanocontacts at both ends of nanotubes; it is flexible and controllable and may be combined with other technologies. It is also obvious that this technology can be used as a method to fill nanotubes with other metals.

3. Nanowires in nanotubes

A nanotube is a one-dimensional nanocontainer that can be filled with various compounds: metal oxides (PbO_2, CoO, PbO, V_2O_5, Bi_2O_3, MoO_3), salts and acids (KI, $AgNO_3$, $HAuCl_4$, H_2PtCl_6, $ZrCl_4$, CsCl, UCl_4, $ThCl_4$, HNO_3, $PdCl_2$, *etc.*), elements (S, Se, Sb, Ge, B) and metal carbides (Mg, Ni, Mn, Nd, Mo, Ta, Co, Cu, *etc.*). Filling can occur both during the synthesis of nanotubes and after the isolation and purification of the preformed nanotubes. The latter way is virtually always more reliable, controllable and target-oriented. Filling can be performed from a gas or vapour phase, from solutions and melts. In nanotubes, as in nanoreactors, chemical synthesis can be carried out (see the review by Rakov [26]).

Of considerable interest is the filling of nanotubes with metals in order to obtain metallic conductors, *i.e.*, nanowires coated with a carbon 'cloth'. In this case, the nanotube not only shapes a nanowire but also protects it from oxidation and deteriorating effects of other corrosive media. It is clear that such nanoobjects are of particular importance from the viewpoint of high technologies.

In early studies on the synthesis of nanotubes containing Cu, Ni, Fe, Ag, Au, Pd and Pt, nanotubes were filled with metal oxides or chlorides which were subsequently reduced with hydrogen into the corresponding metals.[31] Nanowires of β-Sn were obtained by electrolysis of a $LiCl-SnCl_2$ melt that filled a nanotube.[32] Electrolysis was also used to obtain 40–90 nm-long nanowires of a Sn/Pb alloy.[33]

The nanowires formed are usually polycrystalline; however, single-crystal wires were obtained in certain cases. For example, reduction with hydrogen of $Bi(NO_3)_3$ introduced into a single-layer nanotube from a solution in nitric acid gave single crystals of Bi hundreds of nanometers long and with a diameter of about 1 nm in high yield.[34] Unlike a macrocrystal, the nanocrystal obtained in a nanotube was slightly skewed (the planes are inclined). It is of interest that the diameter of a Bi-nanowire is considerably smaller than the diameter of a nanotube; on average, there are five Bi atoms in the tube cross-section. Filling nanotubes ($\sim$ 10 nm diameter) with gaseous $Ni(C_5H_5)_2$ results in a Ni wire with a diameter of 4 nm and a length up to 500 nm.[35] It has not yet been understood why the diameter of the wire formed is so small, especially as the nanowire and nanotube diameters often coincide.

The incorporation of C_{60} fullerene molecules in nanotubes is an exotic event.[36] Such structures resemble 'pods' filled with 'peas', *i.e.*, C_{60} molecules from the gas phase. They are clearly visible under an electron microscope. If filling is incomplete, the fullerene molecules are grouped in twos, threes, *etc.*; they readily move along the tube jumpwise (the jump length ranges from 1 to 10 nm). A jump occurs almost instantaneously (in fractions of a second); the interval between the jumps is 10–20 s. The jumps are induced by electrons emitted by the electron microscope used for observation.

If a 'fullerene-in-a-nanotube' system (C_{60}@NT) is externally doped with metallic potassium, it acquires metallic conductivity owing to the chemical transfer of electrons from potassium to the nanotube and then to C_{60}. As a result, each C_{60} molecule acquires the $6-$ charge, and a compact chain of such molecules inside the nanotube constitutes a nanowire of an organic metal.[37] It is hard to predict the place of such wires in nanotechnologies, but one of its advantages is obvious: it is possible to control charges and their mobilities by the Coulomb fields of external ions (outside the nanotube).

Even more interesting are nanotubes filled with endofullerenes. For example, the La@C_{80}@NT and Gd@C_{82}@NT systems have already been obtained.[38] In these structures, metal ions carry positive charges, whereas the surfaces of the nanotubes are most likely negatively charged.† These are new one-dimensional crystals, the properties and technological 'capabilities' of which are far from being studied completely and are therefore not yet recognized.

A new type of nanowire has recently been obtained. This is a nanocable in which the internal conductor is an iron rod about 10 nm thick and about a micron long 'dressed' with a boron nitride tube with a diameter of about 50 nm.[39] The BN ceramic is an excellent electric insulator, which reliably protects the inserted iron rod from oxygen and other corrosive media. A remarkable feature of these nanocables is that there is a carbon layer between the BN shell and the iron rod; this layer keeps iron in its reduced state and ensures a strong bond between the metal and the ceramic shell. The 'mediation' of carbon is particularly important, considering that BN ceramics are very poorly wetted with iron and their direct contact is very unstable.

The BN nanocables were obtained in an induction graphite furnace from $B_4N_3O_2H$ and an aqueous solution of $Fe(NO_3)_3$ through which a stream of N_2 was passed. Upon heating, $B_4N_3O_2H$ decomposed to give the boron oxides B_2O_3 and B_2O_2. Furthermore, synthesis of CO occurred in the graphite furnace according to the reaction

$$C + H_2O \longrightarrow CO + H_2 .$$

The resulting boron oxides entered the reaction zone at 1700 °C and reacted with the gas mixture $N_2 + CO + H_2$, whereas the $Fe(NO_3)_3$ that was present decomposed to give α-Fe. These reactions resulted in BNFe nanotubes. An electron-microscopic image of one of them is shown in Fig. 5.

It was shown by electron energy loss spectroscopy (EELS) that the outer shell of a nanocable contains only B and N atoms; carbon appears nearer to the centre and its concentration in the B–N–C system is higher nearer the α-Fe nanowire. Such high-conductivity ferromagnetic nanowires that are well protected by ceramics may find a well-deserved application in future nanotechnologies. It should be noted that this technology makes it possible to obtain nanocables containing not only Fe nanowire but also other metals.

† It should be noted that negative charges in C_{60}@HT structures are concentrated inside the tube (on C_{60}^{6-}).

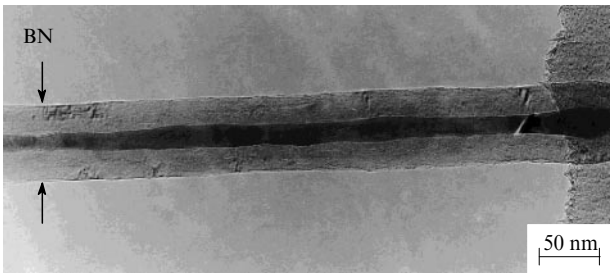


Figure 5. An electron-microscopic image of an iron nanowire (black band) inside a BN nanotube.

4. Nanotube as a field emitter

Perhaps the use of nanotubes as field emitters is their most widespread application. Field emission is emission of electrons from high-curvature surfaces (edges, blades, undulations) under applied voltage. The advantages of field emitters over thermal emission cathodes are well known: these are their small size, low energy consumption, high current density and a possibility of miniaturisation. No wonder that their small radius of curvature, high length/radius ratio, high conductivity and thermal stability make nanotubes a promising emitting material.

The first studies on emission from nanotubes were carried out by Chernozatonskii *et al.*[40] in 1995. Over the short time that has passed since then, working colour displays with diagonal axes of 10 – 20 cm, high luminosity (up to 800 cd cm^{-2}) and long service life have been created. The working elements in such displays consist of nanotubes grown on porous silicon, mesoporous aluminosilicate or quartz using the technologies described above (in the section devoted to the architecture of nanotubes).[41] Displays based on nanotubes will shortly become a market product; this will be the first breakthrough of nanotechnologies in the economy.

Using electron holography, the electric field of a nanotube was studied as a function of potential. This method is based on the interferometry of electrons that have passed through the electric field of a nanotube.‡

A scheme showing the instrumented set up is shown in Fig. 6. A nanotube was mounted on the holder in the electron microscope chamber using a conductive epoxy resin. A current-collecting gold plate was placed opposite the nanotube at a distance of 6 μm from it. A piezoelectric handling device was designed specially for mounting nanotubes.[42] The nanotube and the plate formed an electric circuit to which a voltage V_b was applied. The current in the chain was recorded continuously.

‡ This brilliant technique is used to measure internal potentials, electrostatic and magnetostatic fields, contact potentials, *etc*.

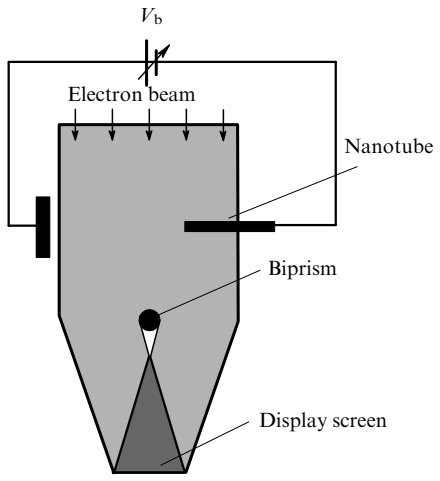


Figure 6. A scheme for the measurement of the electric potential of a nanotube using electron interference.

In the centre of the microscope electron beam, a biprism was placed, which divided the beam into two parts that were later brought together on a display screen at the bottom. The electron field emission of the nanotube manifested itself at a bias voltage of $V_b = 70$ V; the current between the nanotube and the plate was 40 pA. At $V_b = 120$ V, the current was already considerable, *viz*., 0.54 μA, and a holographic picture of the nanotube electric field appeared on the display screen (Fig. 7). The holographic picture shows distinct interference bands along the nanotube (especially in the lower, increased image).

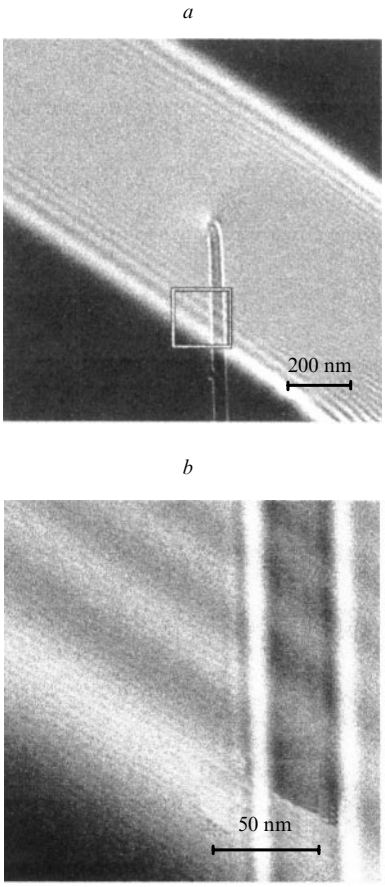


Figure 7. A holographic image of the nanotube potential (*a*) and an enlarged image of the portion marked by the square (*b*).

The observed interference bands appear because the phase of the coherent electron beam which passes near the tube is changed in the electric field of the tube. Superposition of this beam with the other beam which was not exposed to the field of the nanotube results in interference. By analysing the phase shift as a function of the voltage V_b, it is possible to reconstruct the electric field maps around the nanotube (see Fig. 8). Based on these maps, one can find the electric field strength at the tube end (H).[42] The results of this experiment are shown below.

V_b /B	120	90	70
H /B nm^{-1}	1.22	0.82	0.64

It is remarkable that almost the entire electric field is concentrated at the tube end, whereas no other possible sources contribute to the field emission of the nanotube. Given a constant potential V_b, the local electric field at the top of a tube is inversely

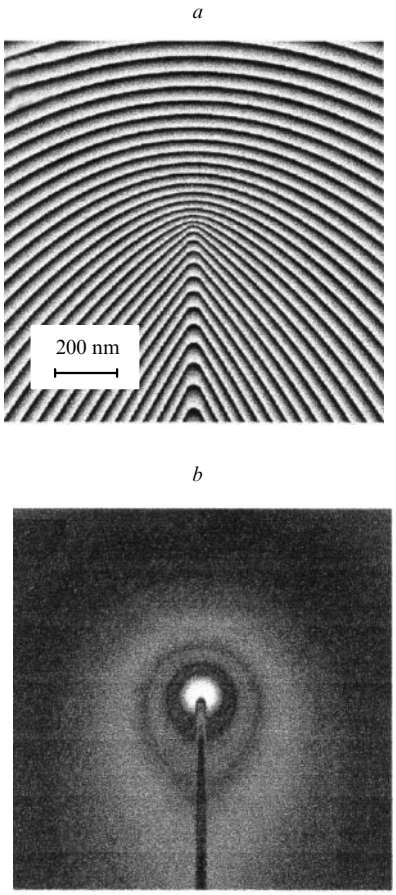


Figure 8. Images of the phase shifts (*a*) and phase gradients (*b*) of the electric potential at the end of a nanotube.

proportional to its radius and almost does not depend on the magnetic field. What is more, the holographic picture confirms that there is no potential drop along the tube even in a strong emission mode. Both of these circumstances, *viz*., localisation of the electric field at the top of the tube and the absence of field gradient along the tube, make nanotubes a perfect material for field displays.

It should be noted that the advantages of the nanotechnological experiments involve not only the gathering of direct information about the properties and behaviour of nanoobjects but also acquiring experience in handling these objects and creating new, sometimes sophisticated, technologies for operating with such objects.

The emission properties of nanotubes can be tuned. For example, filling tubes with cesium decreases the work function by 2 eV; as a result, the emission current increases by an order of magnitude.[43]

Recently, the thermal conductivity of carbon tubes was measured: it is 250 W m^{-1} K^{-1} at room temperature for one-layer tubes and about 3000 W m^{-1} K^{-1} for multilayer tubes. Since the dependence of thermal conductivity on temperature has the form $f(T^2)$, this means that 'two-dimensional' phonons are responsible for thermal conductivity; the free-pathlength of these phonons was estimated to be 500 nm.[44]

The thermostimulated electromotive force (thermo-EMF) generated by a single multilayer nanotube linearly increases with temperature, with a constant gradient of 80 μV K^{-1}; its sign is positive, *i.e*., the thermo-EMF is created by 'holes'.[44]

5. Nanotubes as molecular diodes

Electric conductivity is the key property of nanotubes as elements of nanoelectronics. It is measured by the four-probe method as follows: four conductors [*e.g*., consisting of tungsten obtained from $W(CO)_6$ in a gas phase] are deposited on a nanotube lying on a support in such a way that the distances between the contacts are tens of nanometers. After that, the current–voltage characteristics of the nanotube are measured.

One-layer tubes with the indices (*n*,*n*) are metallic. Perfect tubes (without defects and admixture atoms) have ballistic conductivity: at low resistances of the metal–tube contacts, the resistance of the tube should approach half of the quantum limit of resistance h/e^2 (where h is the Planck constant and e is the electron charge), *i.e*., reach 6500 Ω. However, this limit could not be reached because of the high resistance of the contacts (several megaohms), which creates a Coulombic blockage. Of the metals tested, the best results were obtained for Ti: the Ti–tube nanocontacts have the lowest resistances.[28] At 2 K and nanotube length of $\geqslant 3$ μm, the resistance was about 12 kΩ.

The resistance of such tubes is almost independent of temperature. Similarly, there is no explicit dependence on the bias voltage: when the blocking voltage changes from −100 to 100 V, the nanotube resistance changes only 2–4-fold and the tubes remain conductive. All of these are reliable indications of the 'metallic' behaviour of nanotubes.

Chiral nanotubes with indices (*m*,*n*) are semiconductors with the band gap $E \sim d^{-1}$, where d is the nanotube diameter. For nanotubes with diameters of 0.7 to 3 nm obtained by chemical deposition onto catalytic islands (see Sections III.1 and III.2), the band gap was from 1 to 0.25 eV, respectively. Dai *et al*.[28] thoroughly measured the electron transport properties of one-layer nanotubes obtained by this method. Their resistances at room temperature were 200–500 kΩ for tubes with $d > 2.0$ nm; the resistances were higher (about megaohms) for tubes with smaller diameters ($d < 1.5$ nm). Semiconductor tubes are hole-doped; their conductances decrease when a positive blocking voltage is applied. At 4 K, tubes with $d > 2.0$ nm become insulators in the range from ±10 to ±1000 mV. For tubes with smaller diameters, this range is broader.

A remarkable feature of all $I-V$-dependences for semiconductor tubes is that these characteristics are asymmetrical with respect to the bias voltage and its polarity: at a constant blocking voltage, the absolute current is higher at a positive bias than at a negative bias. The asymmetry increases abruptly as the blocking voltage increases, a feature that is known to characterise a semiconductor diode (rectifier).

Unambiguous evidence that a doped nanotube is a diode was obtained.[45] A one-layer nanotube contaminated with an admixture deposit on certain areas was provided with three Au electrodes (A, B and C, Fig. 9) in such a way that the tube segment between the electrodes B and C is clean, whereas the region between the electrodes A and B contains the impurity deposit (it is clearly visible near the electrode A). The entire device was arranged on a silicon substrate filled with an insulating SiO_2 layer 100 nm thick in such a way that the substrate worked as a capacitive blocking electrode. Resistances were measured in the range from 0.5 MΩ (for metallic tubes) to 10 MΩ (for semiconductor tubes). The contact resistances measured using the four-probe method were ∼0.5 MΩ.

Figure 9*b* shows the $I-V$ -characteristics of the electronic circuit shown in Fig. 9*a*. The inset shows the $I-V$-dependence for the 'non-contaminated' region of the tube (BC): it is symmetrical with respect to the bias potential, *i.e*., the conductivity does not depend on the sign of the bias voltage, which is a feature of a homogeneous semiconductor with distributed *p*- and *n*-carriers. The $I-V$-dependence for the 'contaminated' region AB is strongly asymmetric and depends on the sign of the bias voltage, which is typical of diodes. Thus, the AB region of a nanotube is a molecular diode where the admixture acts as an *n*-type dopant and where an electron–hole junction with a junction potential appears. If the blocking voltage is positive, the current passing through the nanotube decreases. This suggests that holes dominate in the charge transport through the diode.

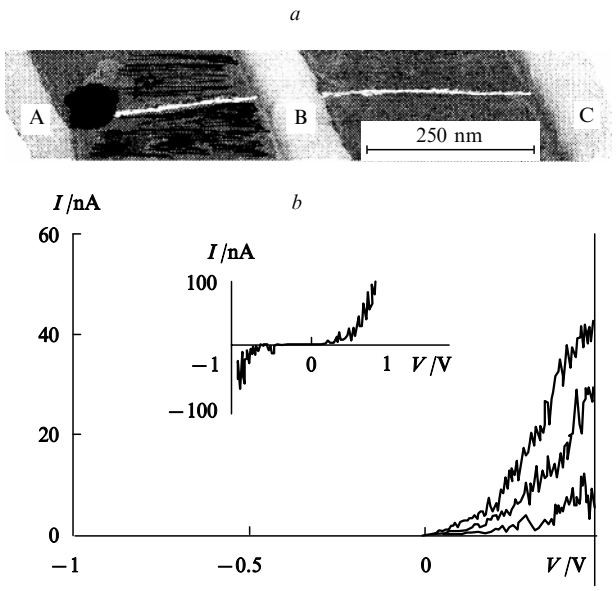


Figure 9. Image of a one-layer nanotube with attached electrodes A, B, C in an atomic force microscope (*a*) and dependence of current in the tube on the bias potential (*b*).

What is more, it turned out that current depends on the blocking voltage in a stepwise manner, *i.e.*, there are discrete zones in a doped nanotube. The following dopant types are possible: admixtures (like amorphous carbon or catalyst clusters), topologic defects (five- or seven-membered rings in the structure of a tube), incorporated atoms (N, B, *etc.*), contacts between tubes with different diameters, mechanical strain of a pipe where it is bent, *etc*.

Of great interest is the controlled doping of nanotubes using the tip of a tunnelling microscope or an atomic pump. It allows one to design flexible hetero-junctions (diodes, transistors) with controlled band structures. Diodes with a slope of $\partial I/\partial V \approx$ 200 nA V^{-1} have already been obtained. The slope normalised with respect to the tube diameter (*i.e.*, to the channel width) is $\sim$0.1 mS μm^{-1}, which is comparable with the slope for a silicon diode.[28] Certainly, we do not speak of immediate replacement of the comprehensively developed silicon electronics by nanoelectronics; however, one can speak of a new direction, *viz*., nanoelectronics (or molecular electronics) with its new advantages. The results of the studies described above allow ways to bring these potential capabilities into reality to be explored.

6. Superconductivity of nanotubes and cryoelectronics

Superconductivity of a bunch of one-layer nanotubes arranged in parallel (about 350 pipes with 1.4 nm diameter each) connected to an electric circuit by ordinary (non-superconducting) Al_2O_3/Pt/Au contacts with layer thicknesses of 5, 3 and 200 nm, respectively, was first discovered by Kociak *et al.*[46] The resistance of such a bunch at 300 K was $\sim$10 kΩ and increased with a decrease in temperature from 300 K to 1 K; after that, an abrupt decrease in resistance occurred (by two orders of magnitude) to a limiting value of 74 Ω at 100 mK. For an electric chain with normal (non-superconducting) contacts, the minimum resistance should not be smaller than half the quantum resistance limit h/e^2; it follows that about 25% of the total number of the tubes (350 tubes) participate in superconductivity. (As expected, a magnetic field of about 1 T destroys superconductivity.)

Taking into consideration the miniature size of electronic nanodevices and the moderate cost of cooling such devices, it can be considered that the superconductivity of nanotubes, nanocontacts and nanowires, even if it appears only at very low temperatures, can be introduced in practical nanoelectronics. This is one of the advantages of cryoelectronics. Yet another advantage of cryoelectronics is the infinitely low noise level.

The discovered superconductivity is similar to that observed in graphite intercalated with alkali metals or in alkaline salts of fullerenes. However, the superconductivity temperature in nanotubes is much lower, which may be attributed to lower-frequency phonons in nanotubes (it is assumed that these phonons correspond to deformation oscillations of nanotubes).[47]

Later,[48] the superconductivity of a single one-layer tube bridging two Au – Ti contacts was discovered. Figure 10 shows how the resistance of such a tube depends on temperature and how superconductivity is destroyed by magnetic fields.

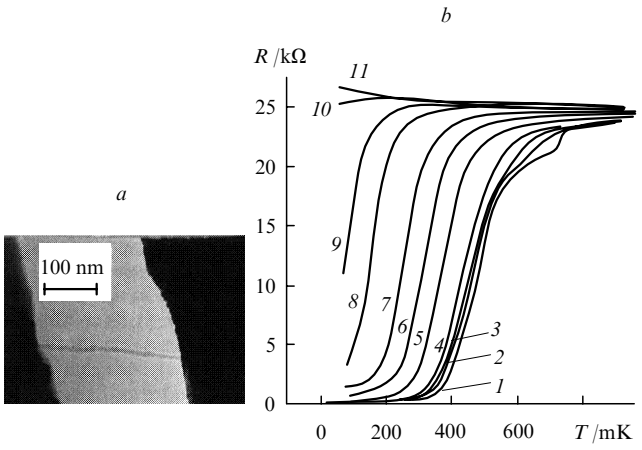


Figure 10. Arrangement of a single nanotube between Ti- and Au-contacts (*a*) and dependence of resistance on temperature in different magnetic fields at I = 1 mA (*b*).
Magnetic field strength /G: (*1*) 0, (*2*) 500, (*3*) 1000, (*4*) 2000, (*5*) 3000, (*6*) 5000, (*7*) 7000, (*8*) 10 000, (*9*) 12 000, (*10*) 15 000, (*11*) 20 000.

IV. Nanowires

Below, we consider 'free' (not enclosed in a carbon nanotube), conducting or light-emitting (metallic or semiconducting) nanowires.

1. Metallic wire

The most developed technique is drawing the wire from nanorods fastened between the cantilever and the tip of a tunnelling microscope.

Figure 11 *a* displays the scheme of a device for drawing nanowires. Gold nanorods (cylinders 0.125 μm in diameter and 2 μm long) were fastened between the gold tip of a tunnel scanning microscope and the tip of an auxiliary microscope. This arrangement enables the simultaneous detection of the electric conductivity and deformation force as a function of the stretch (length) of the nanowire.[49] The dependence of the conductivity and deformation force on the displacement (wire stretching) is shown in Figs 11 *b*,*c*, respectively.

It is interesting to note that electric conductivity and force change in a jump-wise manner: with an increase in length, the former decreases to a limiting value which corresponds to the quantum limit of conductivity.§ The jump-wise behaviour of force means that the wire cross-section changes in a discontinuous manner; jumps occur when atoms rearrange and 'jump into' the final monoatomic chain. The molecular dynamics simulation of an atomic cluster during its stretching (Fig. 11 *d*) perfectly repro-

§ The quantum limit of conductivity is the conductivity of one (monoatomic) tunnelling channel.

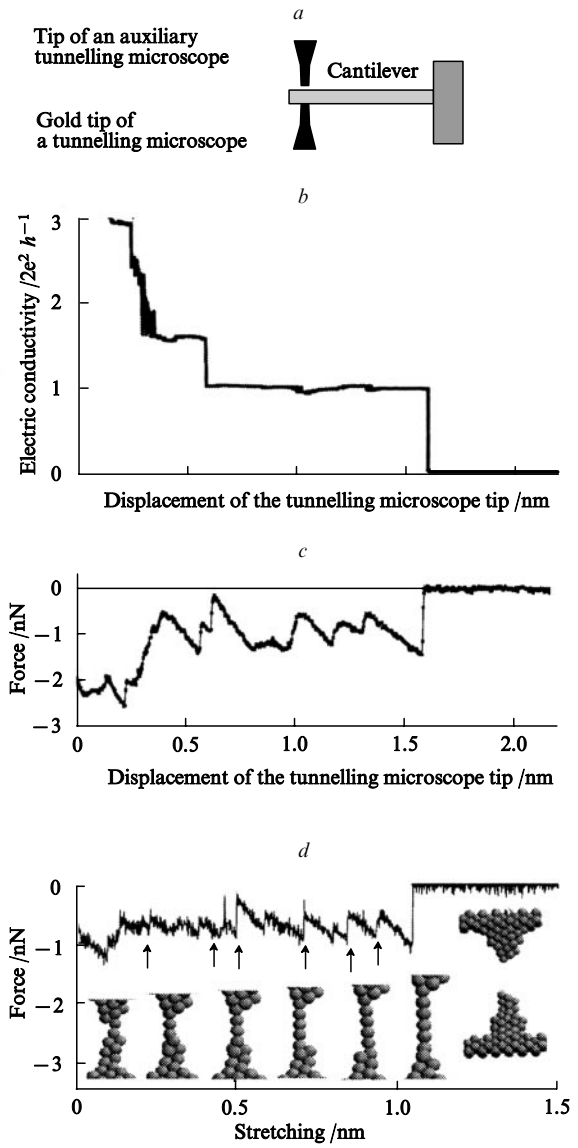


Figure 11. A scheme of a device for drawing nanowires (*a*) and dependence of electric conductivity (*b*) and deformation force (*c*) on displacement. The lower drawing (*d*) shows the results of a molecular dynamics simulation of force as a function of displacement and a scheme of the arrangement of atoms in a nanowire.

duces the experimental dependences. Quantum-chemical calculations within the framework of the density functional theory confirmed the stability of monoatomic chains.¶ It follows from dynamic and quantum-chemical calculations that the degradation occurs in a five-atom linear chain [50] and requires a force of 1.5 ± 0.3 nN. It follows that the energy of an atom–atom bond in a monoatomic chain is twice as high as the atomic bond energy in the bulk metal. This is a reasonable result as a metal features multi-centred bonds and each of such bonds is weaker than a localised and isolated bond.

2. Semiconducting wires and nanolasers

Semiconducting nanowires are usually grown on clusters of metal catalysts. For example, GaP wires with controlled diameters (10, 20 and 30 nm) and > 10 μm long were obtained on gold clusters.[51] Both types of clusters (GaP and Au) were obtained by laser ablation; a direct relationship between the Au cluster size and the diameter of GaP wires was observed, *i.e.*, the wire diameter 'tuned' to fit the size of the catalytic cluster.[52]

Nanowires of GaN,[53] SiC,[54] Ga_2O_3,[55] *etc.* have been obtained to date. A simple technology has been developed to synthesise Ga_2O_3 by heating GaAs with sputter-deposited Au at 1240 °C in a stream of dry O_2; nanowires or nanostrips were obtained, depending on the technology used.[56] Nanowires are single-crystalline; they grow in a direction perpendicular to the (102) plane and display good photoluminescence characteristics. Wu *et al.*[57] synthesised GeO_2 nanowires with 50–120 nm diameters and hundreds of micrometres long. They luminesce upon photoexcitation; the quantum yield of their radiation is an order of magnitude higher than that for GeO_2 powders. A few other types of nanoobjects have recently been obtained, *viz.*, SnO_2 nanowires and nanotubes,[58] silicon nanowire 'wrapped' in a monolayer of gold atoms,[59] nanowires with the composition $Mo_{1-x}W_xS_2$ ($x < 0.1$) (one- and multilayer) with a bamboo trunk-type tubular architecture.[60]

The high yield of optical radiation in semiconductor nanowires stimulated the search for strong nanoemitters that would work as coherent light sources (nanolasers and optical nanowaveguides). The first success was achieved with ZnO nanowires: excitation of densely packed nanowires resulted in laser emission (from the entire set of wires).[61] A more detailed analysis of laser emission from individual nanowires was made by Johnson *et al.*[62] ZnO nanowires were grown on the sapphire (110) surface. This plane is well compatible with the ZnO (0001) plane. ZnO nanowires grown vertically on sapphire were ultrasonically removed from the support and deposited on quartz from an ethanolic solution; their packing density on a horizontal surface was about 300 wires per 1 mm^2.

The wire diameters could be varied from 40 to 150 nm, and their lengths, from 4 to 10 μm. Each wire was detected separately. The laser emission was monitored using a near-field scanning optical microscope combined with fiberglass detection.

The majority of nanowires demonstrated intense light emission localised at their ends; however, they did not show the main sign of laser generation: the generation threshold was not reached even at very high excitation power (above 1 MW cm^{-2}). However, certain nanowires behaved as 'honest' nanolasers: they gave high quantum yields and generation thresholds even at low pumping strength (Fig. 12).

To explain this laser-related 'personality' of nanowires, Johnson *et al.*[62] devised a very plausible explanation: when the wires are ultrasonically detached from the sapphire, their end surfaces are formed in an arbitrary manner, hence light reflecting properties are poor (strong diffusion, phase detuning). This means that the Q value of such 'maimed' nanowires is low. Only part of the wires have well-reflecting ends (*e.g.*, if a nanowire is 'torn out' with

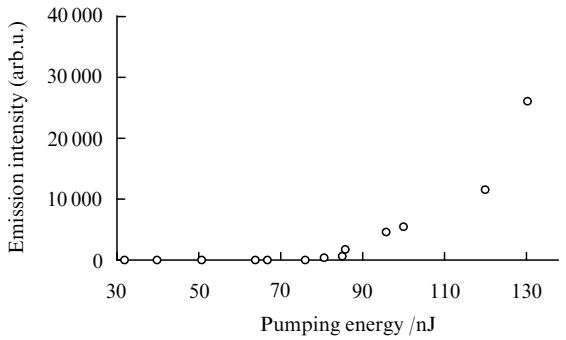


Figure 12. Generation intensity of ZnO nanolasers as a function of pumping energy.

¶ In this context, one has to remember G A Razuvaev who, as early as in the 1970s–80s, synthesised polyatomic metal chains using organometallic chemistry methods.

a nanopiece of sapphire) and hence behave as optical resonators. This is an important result that clearly shows the weaknesses in the technology and suggests ways to overcome them in order to make nanolasers with a low lasing threshold.

3. Ferromagnetic wires

It is considered that ferromagnetic nanowires may become the main elements of quantum magnetic disks, which are the subject of intense development by researchers in the field of nanochemistry. Discrete one-domain elements with high length/diameter ratios, arranged like columns and incorporated in a non-magnetic support, may serve as building blocks for a big information and operation system. Each such block carries one bit of information, and their density reaches hundreds of gigabytes per square centimetre.[63]

The first steps in this direction have already been made:[64] cobalt was electrochemically deposited on anodised aluminium with high pore density (pore diameter 60 nm, density $10^{10}-10^{11}$ cm^{-2}); it filled all the pores to form a regular hexagonal surface 'lattice' of nanowires (columns $\sim$ 60 nm in diameter and 1.6 μm high). This system is essentially a prototype of a quantum magnetic disk. Studies of this system by magnetic force spectroscopy confirmed that each nanowire incorporated in a pore is a one-domain magnet with strong magnetisation anisotropy (Fig. 13). The easy magnetisation axis is oriented along the nanowire. In this direction, the Co wire is a soft ferromagnet, while in the transverse direction, it is a hard ferromagnet as the hysteresis loops suggest.

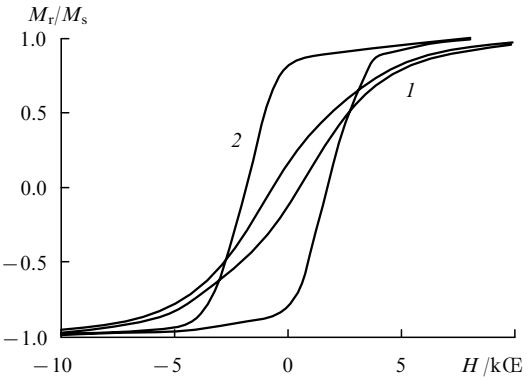


Figure 13. Hysteresis loops of magnetization of a Co nanowire parallel to the long axis (*1*) and perpendicular to it (*2*).

It was shown by magnetic force spectroscopy that the topography of the ferromagnetic columns matches exactly the topography of pores in the starting anodised aluminium, *i.e.*, one nanowire is trapped in each pore. The number of south magnetic poles exactly equals the number of north poles, and all the poles are arranged in a strictly regular manner: each south domain is surrounded by north domains, and vice versa. Magnetic field (1 T) causes complete magnetic orientation of all domains. Such a device is almost ready for recording and reading information (*e.g.*, using the tip of a magnetic force microscope).

It should be noted that the porous structure and hence the topology of ferromagnetic domains are sensitive to electrochemical anodisation and deposition modes, *i.e.*, the quality of nanomagnetic materials can be controlled technologically. There is no doubt that this area of nanochemistry has a great future.

V. Nanomechanics

Handling nanoobjects requires that their mechanical properties are known. The interest in nanomechanics stems from the possibility of creating nanopistons, nanosyringes, nanopumps (*e.g.*, for cell biology), variable capacitance nanocapacitors, nanotweezers and other devices.

1. Internal friction in nanotubes

The first device in which the inner part of a multilayer carbon nanotube moved along an external part (as a piston in a cylinder) was created in 2000.[65] The authors opened the end of a multilayer nanotube and attached a nanomanipulator to the inner tubes. After that, they partially pulled the inner part out while observing this action under an electron microscope.

The first significant result of this work was the creation of a new nanomanipulator. Another result is the observation that, after the pulled-out part of the tube was released by the manipulator, it was instantly retracted back by the restoring force of the van der Waals interaction. It follows from this observation that nanotubes enclosed in each other move relative to each other with almost no friction and thus make an ideal wear-resistant molecular plain bearing.

Direct measurements of the force of cohesion between two coaxial nanotubes were carried out using an atomic force microscope.[66] An individual multilayer nanotube was fixed between the rigid cantilever of a spectrometer and the tip of the upper cantilever of an atomic force microscope (the latter served to measure the length and force). The distance between the cantilevers after stretching the nanotube and the stretching force were recorded.

The experiment was designed to consist of two stages. It was anticipated that disruption of the outer tubes would occur in the first stage due to stretching and that intact inner tubes would slide from under this 'wreckage' upon subsequent stretching.

However, of the 16 experiments that have been carried out, only the first stage, *i.e.*, total destruction of the outer tubes, was observed in 14 cases; it was only in two cases that 'sliding' of inner tubes from outer ones was observed after disruption of the outer tubes. The entire experiment (the measurement of the force F as a function of elongation L) was recorded on video. Analysis of the $F(L)$ relationship gave the cohesion force of sliding nanotubes.[66]

The cohesion force per unit length of the contact was 0.45 and 0.67 N m^{-1} for the two 'successful' experiments (the cohesion force expressed in N m^{-1} corresponds to the cohesion energy expressed in J m^{-2}). It is of note that the interplanar adhesion force in pure graphite is as small as 0.11 – 0.12 N m^{-1}. However, it should be taken into account that the values of 0.45 and 0.67 N m^{-1} are overestimated, as they include not only surface cohesion but also cohesion due to boundary effects, *i.e.*, hindrance of the movement of the inner tube by the broken edges of the outer tube.

2. A nanotube as a high-frequency mechanical oscillator

The negligibly small friction between moving nanotubes opens up a route to nanomechanical oscillators. The mechanical scheme of such an oscillator is shown in Fig. 14.[67]

A block of inner nanotubes that has been drawn out of outer tubes is then drawn back in due to the potential energy $U(x)$ of the van der Waals interaction between the atoms of two sliding tubes,

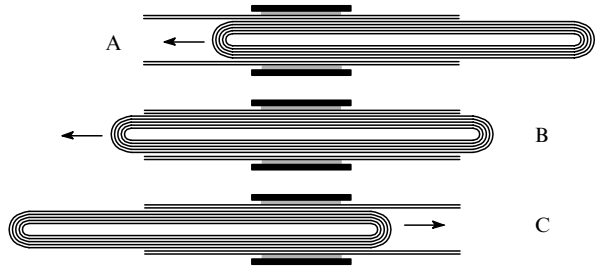


Figure 14. A scheme of movement of inner and outer nanotubes (see the text for comments relating to A – C).

viz., a cylinder and a piston (position A, Fig. 14). When the inner tubes return, the potential energy decreases, whereas the kinetic energy increases: in the equilibrium position B, the former equals zero, whereas the latter has a maximum value. Subsequently, the inner tube is drawn out on the other side because of momentum, until the kinetic energy decreases to zero. At this point (position C), the potential energy acquires a maximum value and draws the tube back in. In fact, this is a typical nanopendulum the oscillation frequency of which can be calculated if the van der Waals restoring force is known. The latter is a function of the displacement of the piston relative to the cylinder.

The van der Waals energy $U(x)$ of the cylinder – piston system was evaluated quantitatively using the Lennard – Jones potential and the structural parameters of the nanotubes (in particular, the gap between the tubes was considered to be 0.34 nm). The oscillation frequency was determined by solving the Newton equation

$$M\,x(t) = F_{\mathrm{vdW}} + F_{\mathrm{fr}}\,,$$

where M is the piston mass; $x(t)$ is the acceleration (the second derivative of the piston coordinate with respect to time); F_{vdW} is the force of the van der Waals cohesion between the piston and the cylinder, which equals $F_{\mathrm{vdW}} = -\mathrm{d}U(x)/\mathrm{d}x$; F_{fr} is the friction force which was considered negligibly small, *i.e*., $F_{\mathrm{fr}} \ll F_{\mathrm{vdW}}$.

Numerical estimates of the oscillation frequency for conditions similar to those used in the experiment by Yu *et al*.[66] gave values of $\sim 10^9$ Hz.

However, it is clear that an external impact is required to start such a gigahertz oscillator (mechanical pendulum). An alternating electric field can serve as the launching system; however, this requires that the piston be electrically charged (this can be achieved, *e.g*., by chemical doping of the nanotubes). In any case, this appears to be a reasonable and promising direction of nanomechanics.

3. A nanopendulum as an electronic shuttle

There is a device known in classical physics, which consists of two big capacitor plates and a metal ball hung between the plates. By applying a DC voltage of several hundred volts to the plates, it is possible to make the ball rock between the plates and transfer charges. The charge carried by the ball in each oscillation is about 10^{10} electrons; the current in the circuit is 1 – 10 μA at an oscillation frequency of about 10 Hz.

In a nanoversion, such a device might work at frequencies of about 100 MHz and carry single electrons. It is quite obvious and realistic that such a device can serve as an element of a quantum computer or a current interrupter in nanocircuits. The first example of a nanopendulum (electronic shuttle) has been reported by Erbe *et al*.[68]

The central part of the device (*a*) (it may be called a quantum bell) and its electrical scheme (*b*) are shown in Fig. 15. Its main part is the turning anchor C, which is (clamped and grounded) fastened in the upper part of a silicon plate. A metal island insulated from the rest of the turning anchor is deposited on its end. The control electrodes G_1 and G_2 carry a voltage (about 3 V) which controls the movement of the anchor-pendulum. The element S supplies electrons, whereas the element D is an electron receiver and plays the role of a FET drain. All the elements are deposited by nanolithography onto a silicon substrate.

The pendulum is brought into motion by an alternating voltage on the electrodes G_1 and G_2 with a frequency f. While moving, the metal island at the pendulum end regularly touches the S and D elements (the space between an element and an island is about 300 nm). The tunnelling of electrons from the element S to the island, and from the island to the element D, occurs during the short moments of contact. The electric capacitance of the contact under static conditions is 84 aF (attoFarads), which corresponds to ±527 electrons at a voltage of ±1 V.

At room temperature, the direct current between the elements S and D is about 20 nA; however, it increases or decreases

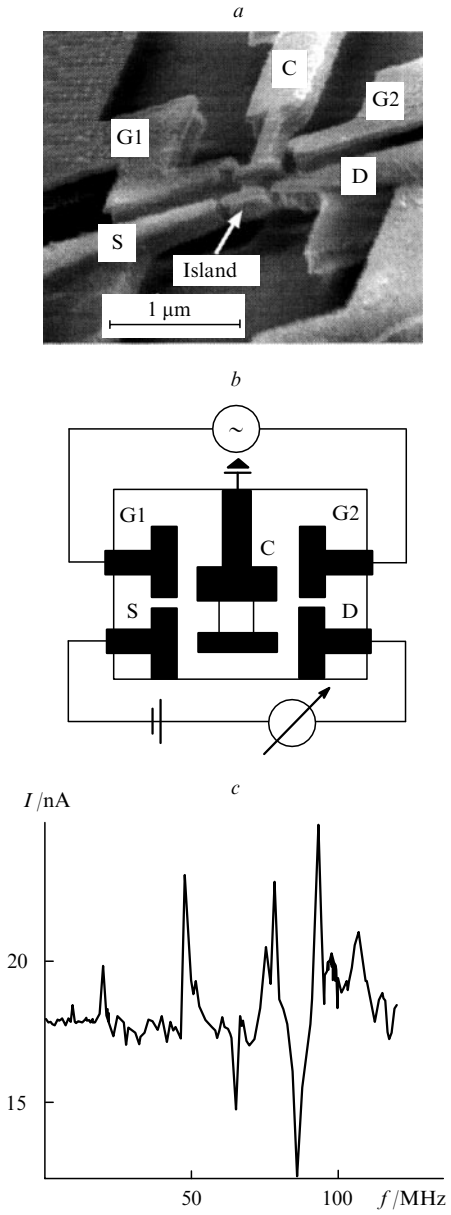


Figure 15. A scheme of a the nanopendulum (*a*, *b*) and the frequency dependence of current transferred by the pendulum at 300 K (*c*) (see text).

abruptly at certain resonance frequencies (see Fig. 15 *c*). Resonance appears at those instants when the frequency of the control current at the electrodes G_1 and G_2 coincides with the intrinsic mechanical frequency of the pendulum. One can see that the range 40 – 120 MHz contains several resonances of this kind, *i.e*., there are several intrinsic frequencies of the pendulum, corresponding to different modes of high-frequency mechanical movement (bending, torsion, oscillation). The anti-resonances (current dips at certain frequencies) appear when the pendulum stops due to non-coincidence between the control frequency and the intrinsic frequency. In total, this mode may be called the 'irregular movement' of a pendulum.

However, as the temperature is decreased, the irregular mechanical modes start to 'freeze out', and only one intrinsic frequency of 120 MHz remains at 4.2 K; the current at this frequency corresponds to the transfer of 0.11 ± 0.001 electrons per pendulum oscillation. This is a pure mode in which the pendulum works as a discrete electron shuttle, transferring one electron on each ninth oscillation from S to D.

VI. Technologies for handling nanoobjects

Nanotechnology comprises two main constituents: (1) creating nanoobjects for nanodevices; (2) operations with these objects and mechanisms for handling them. And although studies along both directions are being carried out astonishingly quickly (similar development rates in the history of science have only been observed in relation to the discovery of superconducting ceramics and 'cold thermonuclear fusion'), the second constituent still remains a weak, limiting point.

In the previous sections, we have already discussed some operating devices and nanomanipulators. Presently, the employment of the scanning tunnelling microscope (STM) and atomic force microscope (AFM) seem the most promising technologies. As Rakov has aptly noted in his paper,[26] 'after the invention of STM and AFM molecular nanotechnology is no longer only a scientific concept'; it may be added that it has moved to the stage of acquiring practical experience.

1. Study of nanotubes and nanorods lying on a surface

The tip of an AFM reveals that nanotubes lying on a surface possess folds, bends, loops and even foldovers. The latter are changes in the lower tube occurring due to the compression force from the upper tube: it deforms markedly (by about 30%), its cross-section becomes elliptic, and the crossing point of the tubes is displaced downwards. By measuring this displacement and using the known Young modulus (about 1.5 TPa), one can evaluate the compression force and the energy of 'adhesion' of the pipe to the surface. For a multilayer nanotube with a diameter of 100 Å that lies on the surface of passivated silicon, the binding energy to the surface is 0.08 eV nm^{-1} (per unit length of the tube). The compression force at the point of contact of two crossing tubes is about 35 nN; this corresponds to a pressure of about 10 GPa.[69] The compression of a one-layer tube with a diameter of 1.3 nm by 30% requires a force of $\sim$10 nN.

The interaction between a nanotube and a surface determines both the normal force and the force of horizontal displacement (pinning), which is responsible for the friction of a tube moving along a support. The pinning force for a nanotube (10–30 nN) is comparable to the force with which the AFM tip affects an object. This possibility of moving nanotubes along the surface by means of an AFM tip has been implemented brilliantly.[69] It is possible to manipulate nanotubes in many ways: they can be moved, bent, twisted, oriented, turned around the normal line relative to the surface and shaped (in particular, Hertel *et al.*[69] shaped nanotubes as the contour of the Greek letter θ). Even an attempt to dissect a nanotube with an AFM tip succeeded, though after prolonged 'dragging' of the tube along the surface.

The mastering of the technology for manipulating nanotubes by means of an atomic force microscope is an important breakthrough in nanotechnology, as it removes barriers (including psychological ones) to the design of systems and ensembles from nanotubes with subsequent 'welding' of the ends with an electron or laser beam. An atomic force microscope was also used to move (rotate and displace) gold nanorods (10 nm in diameter, 70 nm long) on a SiO_2 surface;[70] it was shown that the ease of manipulation depends on the point of application of the force on a nanorod.

An interesting and seemingly promising technology for manipulating nanotubes has been proposed by Kim and Lieber.[71] They 'equipped' a scanning probe microscope with nanotweezers, which are made of two gold leaflets with nanotubes and an insulating glass spacer. By applying a controlled electric field to the plates, it is possible to manipulate the nanotubes and grip nanoobjects with them. By varying the diameters of the nanotubes, it is possible to adapt the nanotweezers for gripping nanoobjects of various sizes.

2. Magnetic field as a manipulator

The spatial orientation and lining up of extended nanoparticles, as well as assembling them into ensembles can be performed by a magnetic field. For example, nanotubes are oriented in a magnetic field in such a way that their long axes are directed along the magnetic field (Fig. 16). The orientational probability (the fraction of nanotubes directed along the field) increases with an increase in the magnetic field.

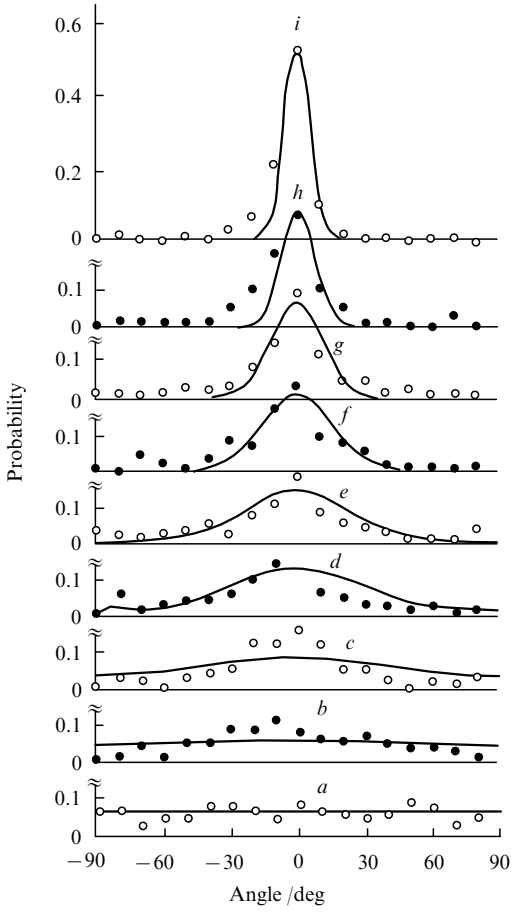


Figure 16. Dependence of the degree of nanotube orientation on the magnetic field strength (H).
(a) 0, (b) 5, (c) 10, (d) 16, e) 20, (f) 30, (g) 40, (h) 60, (i) 80 kŒ.

For multilayer nanotubes (the number of layers is 23 ± 7, the inner diameter is 2.8 nm, the outer diameter is 17.9 nm, the length is 1.5 μm), the anisotropy of magnetic susceptibility measured from the dependence of orientation on the field (see Fig. 16) is $x_{\parallel} - x_{\perp} = (9 \pm 5) \times 10^{-6}$ cm^3 K per mole of carbon atoms contained in a nanotube.[72]

The anisotropy evaluated theoretically (under the assumption that the atomic magnetic susceptibility is the same as that in graphite) is 124×10^{-6} cm^3 K mol^{-1}, which is much higher than that measured experimentally. This discrepancy is convincing proof that there are circular diamagnetic currents induced by the external magnetic field along the axis of the nanotube.

A remarkable (and unexpected) result is the dependence of the susceptibility anisotropy on temperature: at 231 and 314 K, it is 4×10^{-6} and 45×10^{-6} cm^3 K mol^{-1}, respectively.[73] This dependence cannot be ascribed to kinetic effects in orientation mobility: the arrangement of nanoparticles in a magnetic field was always performed under the same conditions, *viz.*, in a CCl_4 solution, at prolonged exposure to the field and with the sub-

sequent fixation of the resulting orientation distribution by removal of the solvent. The origin of this effect remains unclear. It is possibly due to the internal coaxial rotation of tubes relative to each other. The high-frequency rotation of tubes (see the section on nanomechanics) may be the source of extra current and contributes to the anisotropy of magnetic susceptibility.

3. Atomic-molecular pump

A project has been proposed (and there are grounds to consider it highly realistic) involving a laser-controlled atomic-molecular pump in which a nanotube is used as a container for transporting atoms, ions or molecules and for applying them to a surface.[74] For this purpose, it is necessary to create a flow of hot electrons in a tube filled with atoms, ions or molecules (*e.g.*, Li^+ or C_{60}^{6-}); these electrons will 'carry' atoms and ions along the tube. Usual direct excitation is not suitable for these purposes as a nanotube is a molecule with a centrally symmetric potential. In these molecules, the number of hot electrons that move in opposite directions (to the left and to the right) along the tube is the same, *i.e.*, there is no electronic current. Asymmetry in the distribution of 'left' and 'right' electrons can be created by quantum interference of one- and two-photon excitation by coherent light at frequencies of $2\omega_0$ and ω_0. Under such coherent two-frequency excitation, the electronic current appears in the tube, the direction of which is defined by the phase offset between the two laser sources and can be phase-controlled. Such laser-stimulated electronic current was called 'electronic wind' (Fig. 17).

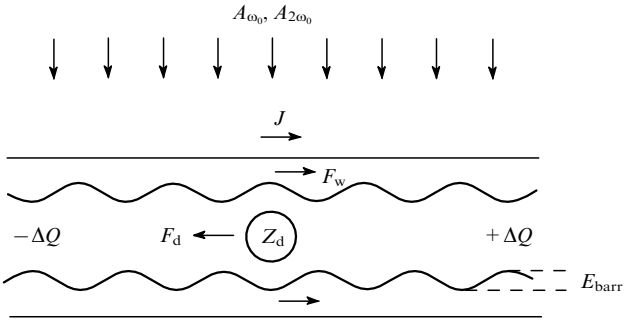


Figure 17. A scheme of a laser-controlled atomic-molecular pump (see text).

If the tube contains neutral (uncharged) atoms or molecules, the elastic scattering of hot electrons on these species will move the latter in the direction of the electronic wind. However, if the tube is filled with partially charged atoms or molecules, then the elastic scattering of hot electrons will create an electrostatic field the potential of which is directed against the electronic wind (see Fig. 17). This occurs because the number of electrons moving along the electronic wind (from the left to the right) is larger than that of electrons moving in the opposite direction. Hence, the number of electrons reflected to the left will be greater than the number of electrons reflected to the right. Thus, the electric charges $\pm\Delta Q$ created by reflection generate a field in which atoms move against the electronic wind.

Theoretical estimates of the operation of such a pump are very optimistic. In fact, for lithium with an effective charge of $+0.6$, the motive force F_d is -0.8 μeV; for a neutral Li atom carried by the electronic wind, the mean rate F_w is 25 nm μs^{-1} (see Ref. 74)

An atomic-molecular pump can be easily controlled by light through phase ratios and intensities. There is no doubt that such a pump will be implemented in the near future. Following that, new breakthroughs in cluster chemistry and nanoelectronics should be expected.

4. Magnetic-resonance atomic-force spectroscopy as a new nanotechnology

The magnetic-resonance atomic-force spectroscopy combines the principles of atomic force microscopy and magnetic resonance. The areas of its application are obvious even now: these include the visualisation of magnetic nanostructures on the atomic scale, measurement of the density of electron magnetic moments and magnetic relaxation in nanostructures, use in spintronics devices (see Section II.4) and in reader elements of quantum computers, *etc*.

The typical elements of a magnetic-resonance atomic-force spectrometer are shown in Fig. 18. A micron-size ferromagnetic tip (made of an $SmCo_5$ or Pr–Fe–B alloy) is fastened at the end of an atomic-force cantilever. The sample to be studied is placed under the tip in a non-uniform field B_z with a vertical gradient dB_z/dz. The external field B_z and the magnetic field of the ferromagnetic tip create concentric surfaces with equal magnetic field strengths (isomagnetic surfaces) in the sample.† A microwave coil is placed aside of the sample; the purpose of the coil is to irradiate the sample at a frequency ω corresponding to the electron paramagnetic resonance.

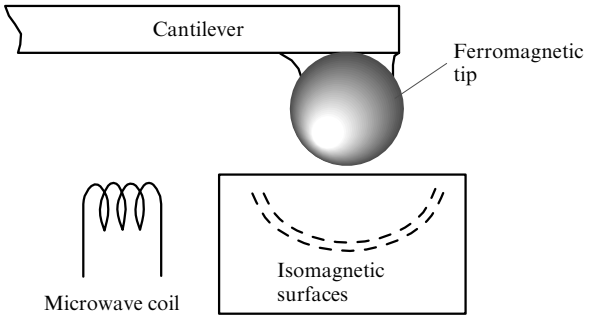


Figure 18. A scheme of a magnetic-resonance atomic-force spectrometer.

Because the magnetic field in the sample is non-uniform, only a small fraction of the spins (only those located on the isomagnetic surface with a field strength B_z) respond to the microwave frequency ω:

$$\omega = \gamma B_z ,$$

where γ is the gyromagnetic ratio for the electron spin. On two neighbouring isomagnetic surfaces separated by a distance Δz, the resonance conditions have the form:

$$\omega_1 = \gamma (B_z)_1,$$
$$\omega_2 = \gamma (B_z)_2.$$

Then, the difference between the resonance frequencies $\Delta\omega = \omega_1 - \omega_2$ is expressed through the field gradient:

$$\Delta\omega = \gamma [(B_z)_1 - (B_z)_2] = \frac{dB_z}{dz}\Delta z.$$

If the resonance bandwidth for electron spins in the sample is $\Delta\omega$, then, at a given field gradient, all the electron spins in the Δz layer undergo microwave resonance.

In a few experiments using magnetic-resonance atomic-force spectroscopy, field gradients (dB_z/dz) of 300–2200 T m^{-1} were used (see Refs 75 and 76); the largest gradient value was

† Note that isomagnetic surfaces are not necessarily spherical (more exactly, hemispherical). The surface shape is defined by the shape of the nanotip and the profile of its magnetic field. A ferromagnetic nanocrystal of any shape can serve as a nanotip.

250 000 T m^{-1} (see Ref. 77). Given a resonance band width of $\Delta\omega = 1$ Hz (this band corresponds to an ESR line width of 1 Hz) and a field gradient of 2000 T m^{-1} (*i.e.*, 2×10^{-2} Hz nm^{-1}), we obtain $\Delta z = 50$ nm. This means that microwave irradiation with the band $\Delta\omega = 1$ Hz can affect the spins of the electrons located in a layer 50 nm thick. At the record gradient of 250 000 T m^{-1} (this is 25 Hz nm^{-1}), the layer thickness is 0.4 nm. It is clear that the stronger the gradient of a non-uniform magnetic field the thinner the layer that is probed magnetically.

Unlike the electron spin resonance technology which detects and measures the microwave power absorbed by an electron spin system, magnetic-resonance atomic-force spectroscopy detects and measures the magnetic force on the cantilever. In this case, microwave irradiation results in reorientation of electron spins (transitions between Zeeman levels occur) and a change in the spin magnetisation of the probed layer in the sample being studied. As a result, the magnetic force on the cantilever changes.

As an elastic system, a cantilever has its own frequency of mechanical oscillations f (about 1–10 kHz, depending on its shape and mass) and elastic constant k (about 10^{-2} N m^{-1}). The oscillation frequency of the cantilever is maintained constant by a piezoelectric element which controls the cantilever movement. The electric field at the control piezoelectric element is created by a fibre-optic interferometer that monitors the position of the cantilever and generates a control signal, which maintains the cantilever's own frequency.

When an external gradient magnetic field B_z is applied, the spin system is polarised (the spins are oriented) and the magnetisation acquires a steady-state value. The magnitude of this magnetisation is determined by two factors: first, the external constant field B_z, and second, the magnetic field of the tip. The magnetic field of the cantilever with a ferromagnetic tip, which oscillates along the coordinate z, varies as a function of the tip's field; simultaneously, the sample layer with thickness Δz also undergoes height-oscillation along this coordinate.

At the instant when the cantilever is at its amplitude maximum, the microwave field is turned on (phase synchronisation). The spin system and spin magnetisation now change for two reasons: first, due to the microwave field that inverts the spins, and second, due to the movement of the cantilever, which changes the positions of the resonance layers in such a way that the spins are either affected by the resonance microwave field or come out of resonance.

In the new steady state (in the presence of a microwave field) a new value of magnetisation is established and the oscillating magnetic force F between the cantilever and the sample changes; as a result, the elastic constant of the cantilever changes and its new own frequency is established. The change in the elastic constant Δk is defined by the relationship

$$\Delta k = \frac{F}{\Delta a},$$

where Δa is the cantilever's oscillation amplitude (normally about 20 nm) and

$$\frac{\Delta f}{f} = 0.5\,\frac{\Delta k}{k}.$$

This allows one to determine the oscillation part of the magnetic force F, which is a function of the number of spins being detected, the amplitude of the microwave excitation and the relaxation time of spin magnetisation. The sensitivity of this technology is as high as a hundred electron spins in a nanometre layer.[77]

Thus, a magnetic-resonance atomic-force spectrometer is a superdynamic system that analyses the behaviour of two dynamic interacting subsystems: (i) a spin subsystem in a microwave field and in an oscillating field of a cantilever and (ii) a mechanical oscillating subsystem of the cantilever, which modulates the spin subsystem.

Of course, this new technology is still in its infancy; it operates under high vacuum conditions and at cryogenic temperatures and is still 'aristocratic'. However, its potential for studying the 'nanoworld' is huge.

* * *

Being the chemistry of nanoobjects, nanochemistry is inseparable from nanotechnologies as a combination of methods for handling nanoobjects. This field of chemistry has tempting prospects; some of these are already being implemented, while others are on the 'waiting list'. And, though making predictions is the same as writing memoirs for a person who has just been born and then making that person live according to those memoirs, it may be stated with certainty that nanochemistry and nanotechnologies will some day become as important as life chemistry.

References

1. A L Buchachenko, F I Dalidchik, S A Kovalevskii, B R Shub *Usp. Khim.* **70** 611 (2001) [*Russ. Chem. Rev.* **70** 535 (2001)]
2. F I Dalidchik, S A Kovalevskii, B R Shub *Usp. Khim.* **70** 715 (2001) [*Russ. Chem. Rev.* **70** 627 (2001)]
3. J Gaudioso, W Ho *J. Am. Chem. Soc.* **123** 10 095 (2001)
4. A L Buchachenko *Usp. Khim.* **57** 1593 (1987) [*Russ. Chem. Rev.* **57** 907 (1987)]
5. I S Antipin, E Kh Kazakova, V D Khabikher, A I Konovalov *Usp. Khim.* **67** 995 (1998) [*Russ. Chem. Rev.* **67** 905 (1998)]
6. G Alberti, S Murcia-Mascaros, R Vivani *J. Am. Chem. Soc.* **120** 9291 (1998)
7. W Lu, S Yang *J. Phys. Chem. A* **102** 825 (1998)
8. A A Heikal, S H Chong, J S Baskin, A H Zewail *Chem. Phys. Lett.* **242** 380 (1995)
9. K Egashira, N Nishi *J. Phys. Chem. B* **102** 4054 (1998)
10. W Christen, U Even *J. Phys. Chem. A* **102** 9420 (1998)
11. G B Sergeev *Usp. Khim.* **70** 915 (2001) [*Russ. Chem. Rev.* **70** 809 (2001)]
12. R D Levine, R B Bernstein *Molecular Reaction Dynamics and Chemical Reactivity* (London: Oxford University Press, 1987)
13. A Berces, P A Hackett, L Lian, S A Mitchell, D M Rayner *J. Chem. Phys.* **108** 5476 (1998)
14. S A Mitchell, L Lian, D M Rayner, P A Hackett *J. Chem. Phys.* **103** 5539 (1995)
15. S A Mitchell, D M Rayner, T Bartlett, P A Hackett *J. Chem. Phys.* **104** 4012 (1996)
16. A Sanchez, S Abbet, U Heinz, W-D Schneider, H Hakkinen, R N Barnett, U Landman *J. Phys. Chem. A* **103** 9573 (1999)
17. R C Bell, K A Zemski, K P Kerns, H T Deng, A W Castleman Jr *J. Phys. Chem. A* **102** 1733 (1998)
18. E R Bernstein (Ed.) *Chemical Reactions in Clusters* (New York: Oxford University Press, 1996)
19. V V Smirnov, in *Problemy i Dostizheniya v Oblasti Nanomaterialov* (Problems and Advances in Nanomaterials) (Moscow: L Ya Karpov Research Physochemical Institute, 2002) Vol. 2, p. 79
20. B O Dabbousi, J Rodriguez-Viejo, F V Mikulec, J R Heine, H Mattoussi, R Ober, K F Jensen, M G Bawendi *J. Phys. Chem. B* **101** 9463 (1997)
21. M R Buitelaar, A Bachtold, T Nussbaumer, M Iqbal, C Schönenberger *Phys. Rev. Lett.* **88** 156 801 (2002)
22. D J Norris, N Yao, F T Charnock, T A Kennedy *Nano Lett.* **1** 3 (2001)
23. Yu I Petrov *Klastery i Malye Chastitsy* (Clusters and Small Particles) (Moscow: Nauka, 1986)
24. S P Gubin *Khimiya Klasterov* (The Chemistry of Clusters) (Moscow: Nauka, 1987)
25. S Wolf, D Awschalom, R Buhrman *Science* **294** 1488 (2001)
26. E G Rakov *Usp. Khim.* **70** 934 (2001) [*Russ. Chem. Rev.* **70** 827 (2001)]
27. P J F Harris *Carbon Nanotubes and Related Structures* (Cambridge: Cambridge University Press, 1999)
28. H Dai, J Kong, C Zhou, N Franklin, T Tombler, A Cassell, S Fan, M Chapline *J. Phys. Chem. B* **103** 11 246 (1999)

29. Y Saito, Y Tani, A Kasuya *J. Phys. Chem. B* **104** 2495 (2000)
30. A Cao, X Zhang, J Wei, Y Li, C Xu, J Liang, D Wu, B Wei *J. Phys. Chem. B* **105** 11937 (2001)
31. J Cook, J Sloan, M L H Green *Fullerene Sci. Technol.* **5** 695 (1997)
32. M Terrones, W K Hsu, A Schilder, H Terrones, N Grobert, J P Hare, Y Q Zhu, M Schwoerer, K Prassides, H W Kroto, D R M Walton *Appl. Phys. A: Mater. Sci. Process.* **66** 307 (1998)
33. T Kyotani, L Tsai, A Tomita *Chem. Commun.* 701 (1997)
34. C-H Kiang, J-S Choi, T T Tran, A D Bacher *J. Phys. Chem. B* **103** 7449 (1999)
35. B K Pradhan, T Kyotani, A Tomita *Chem. Commun.* 1317 (1999)
36. B W Smith, M Monthioux, D E Luzzi *Chem. Phys. Lett.* **315** 31 (1999)
37. T Pichler, H Kuzmany, H Kataura, Y Achiba *Phys. Rev. Lett.* **87** 267 401 (2001)
38. K Hirahara, K Suenaga, S Bandow, H Kato, T Okazaki, H Shinohara, S Iijima *Phys. Rev. Lett.* **85** 5384 (2000)
39. R Ma, Y Bando, T Sato *Chem. Phys. Lett.* **350** 1 (2001)
40. L A Chernozatonskii, Yu V Gulyaev, Z Ya Kosakovskaja, N I Sinitsyn, G V Torgashov, Yu F Zakharchenko, E A Fedorov, V P Val'chuk *Chem. Phys. Lett.* **233** 63 (1995)
41. Y Saito, S Uemura *Carbon* **38** 169 (2000)
42. J Cumings, A Zettl, M R McCartney, J C H Spence *Phys. Rev. Lett.* **88** 6804 (2002)
43. D-H Kim, H-R Lee, M-W Lee, J-H Lee, Y-H Song, J-G Jee, S-Y Lee *Chem. Phys. Lett.* **355** 53 (2002)
44. P Kim, L Shi, A Majumdar, P L McEuen *Phys. Rev. Lett.* **87** 215502 (2001)
45. R D Antonov, A T Johnson *Phys. Rev. Lett.* **83** 3274 (1999)
46. M Kociak, A Yu Kasumov, S Gueron, I I Khodos, Yu B Gorbatov, V T Volkov, L Vaccarini, H Bouchiat *Phys. Rev. Lett.* **86** 2416 (2001)
47. B Reulet, A Yu Kasumov, M Kociak, R Deblock, I I Khodos, Yu B Gorbatov, V T Volkov, C Journet, H Bouchiat *Phys. Rev. Lett.* **85** 2829 (2000)
48. A Yu Kasumov, R Deblock, M Kociak, B Reulet, H Bouchiat, I I Khodos, Yu B Gorbatov, V T Volkov, C Journet, M Burghard *Science* **284** 1508 (1999)
49. G Rubio-Bollinger, S R Bahn, N Agrait, K W Jacobsen, S Vieira *Phys. Rev. Lett.* **87** 026 101 (2001)
50. E Z daSilva, A J R daSilva, A Fazzio *Phys. Rev. Lett.* **87** 256102 (2001)
51. M S Gudiksen, C M Lieber *J. Am. Chem. Soc.* **122** 8801 (2000)
52. J Holmes, K Johnston, R Doty, B Korgel *Science* **287** 1471 (2000)
53. X Duan, C M Lieber *J. Am. Chem. Soc.* **122** 188 (2000)
54. H Dai, E W Wong, Y Z Lu, S Fan, C M Lieber *Nature (London)* **375** 769 (1995)
55. H Zhang, Y Kong, Y Wang *Solid State Commun.* **109** 677 (1999)
56. G Gundiah, A Govindaraj, C N R Rao *Chem. Phys. Lett.* **351** 189 (2002)
57. X C Wu, W H Song, B Zhao, Y P Sun, J J Du *Chem. Phys. Lett.* **349** 210 (2001)
58. Z R Dai, J L Gole, J D Stout, Z L Wang *J. Phys. Chem. B* **106** 1274 (2002)
59. C P Li, X H Sun, N B Wong, C S Lee, S T Lee, B K Teo *J. Phys. Chem. B* **106** 6980 (2002)
60. M Nath, K Mukhopadhyay, C N R Rao *Chem. Phys. Lett.* **352** 163 (2002)
61. M Huang, S Mao, H Feick *Science* **292** 1897 (2001)
62. J C Johnson, H Yan, R D Schaller, L H Haber, R J Saykally, P Yang *J. Phys. Chem. B* **105** 11 387 (2001)
63. R L White, R M H Newt, R F W Pease *IEEE Trans. Magn.* **33** 990 (1997)
64. D H Qin, M Lu, H L Li *Chem. Phys. Lett.* **350** 51 (2001)
65. J Cumings, A Zettl *Science* **289** 602 (2000)
66. M-F Yu, B I Yakobson, R S Ruoff *J. Phys. Chem. B* **104** 8764 (2000)
67. Q Zheng, Q Jiang *Phys. Rev. Lett.* **88** 045 503 (2002)
68. A Erbe, C Weiss, W Zwerger, R H Blick *Phys. Rev. Lett.* **87** 096 106 (2001)
69. T Hertel, R Martel, P Avouris *J. Phys. Chem. B* **102** 910 (1998)
70. S Hsieh, S Meltzer, C R C Wang, A A G Requicha, M E Thompson, B E Koel *J. Phys. Chem. B* **106** 231 (2002)
71. P Kim, C M Lieber *Science* **286** 2148 (1999)
72. M Fujiwara, E Oki, M Hamada, Y Tanimoto, I Mukouda, Y Shimomura *J. Phys. Chem. A* **105** 4383 (2001)
73. M Fujiwara, Y Tanimoto *RIKEN Rev.* **44** 164 (2002)
74. P Král, D Tománek *Phys. Rev. Lett.* **82** 5373 (1999)
75. K J Bruland, J Krzystek, J L Garbini, J A Sidles *Rev. Sci. Instrum.* **66** 2853 (1995)
76. O Züger, S T Hoen, C S Yannoni, D Rugar *J. Appl. Phys.* **79** 1881 (1996)
77. K J Bruland, W M Dougherty, J L Garbini, J A Sidles, S H Chao *Appl. Phys. Lett.* **73** 3159 (1998)